Discover Environment

Research

Geoenvironmental and geophysical methods applied to identify natural attenuation process on a complex hydrogeological environment contaminated by hydrocarbons

Alexandre Muselli Barbosa[1,2] · Leonides Guireli Netto[1,3] · Camila Camolesi Guimarães[1] · João Pedro Silva Pereira[1] · Otávio Coaracy Brasil Gandolfo[1] · Lelia Cristina da Rocha Soares[2] · Claudio Augusto Oller do Nascimento[2]

Received: 19 February 2024 / Accepted: 21 October 2024
Published online: 26 October 2024

Abstract
Environmental contamination found in urban areas generally has a chemical composition that favors the generation of a variety of physical, chemical and biological processes that differ from natural soil parameters. Thus, understanding natural attenuation processes in tropical environments is still a challenge, as is understanding how biogeochemical processes can influence and modify natural soil characteristics. The study aimed to apply methods that are not commonly used in investigations of contaminated areas, in order to assess the applicability of non-invasive methodology for detailed stratigraphic characterization and biogeochemical changes resulting from contamination by hydrocarbons in a complex hydrogeological environment site. To date, few studies have presented results obtained using non-invasive techniques to understand biochemical processes. The research was based on the interpretation of results obtained by high-resolution physical environment characterization techniques (such as gamma geophysical profiling and electrical conductivity surveys) and chemical analysis of groundwater. The data was interpreted to obtain a detailed characterization of the study area and evidence of the occurrence of natural attenuation of creosote contamination. The results indicated that the combination of geoenvironmental and geophysical methods is an interesting alternative for obtaining data and understanding the mineralogical and stratigraphic variation of the contaminated area. The physical parameters variations obtained by the methods suggested the presence of local geochemical alterations resulting from natural processes of attenuation of contamination by aliphatic and aromatic hydrocarbons in a tropical environment. The natural attenuation processes were confirmed through groundwater samples, biological analysis and metagenomic classification.

Keywords Contamination · Creosote · Penetrometry · Natural gamma · Electrical conductivity profiling

✉ Leonides Guireli Netto, leonidesnetto@ipt.br; Alexandre Muselli Barbosa, muselli@ipt.br; Camila Camolesi Guimarães, camilacg@ipt.br; João Pedro Silva Pereira, jpereira@ipt.br; Otávio Coaracy Brasil Gandolfo, gandolfo@ipt.br; Lelia Cristina da Rocha Soares, lelia.cr.soares@usp.br; Claudio Augusto Oller do Nascimento, oller@usp.br | [1]Institute for Technological Research (IPT), Av. Prof. Almeida Prado, 532, Cidade Universitária, São Paulo, São Paulo State 05508-901, Brazil. [2]Department of Chemical Engineering, University of São Paulo (USP), São Paulo, São Paulo State, Brazil. [3]Geosciences and Exact Sciences Institute (IGCE), São Paulo State University (UNESP), Rio Claro, São Paulo State, Brazil.

1 Introduction

Urbanization has been a defining global trend over the past century, with the world's population increasingly concentrated in cities. This rapid urban expansion, driven by industrialization and economic opportunities, has led to significant environmental challenges, particularly in managing land use and contamination in densely populated areas. In Brazil, about 85% of the population lives in urban areas, as documented in the latest national census published in 2010 [1]. This percentage is even higher in the southeastern part of the country, where it reaches 93%. The sharp rise in urban populations can be traced back to the massive wave of urbanization and the migration from rural areas between the 1960s and 1980s, a phenomenon seen not only in Brazil but across many Latin American nations [2]. This accelerated urban expansion gave rise to large metropolitan regions, including São Paulo, which has since become the most populous city in Latin America and a key global megacity in terms of both population and geographical size. São Paulo exemplifies the extensive industrial and urban growth that reshaped South America in the latter half of the twentieth century. With more than 166 inhabitants per square kilometer, the city is under pressure to transform previously unusable land, such as brownfields and other polluted sites, into areas fit for urban use [1]. The rapid pace of urbanization has led to a notable increase in the number of contaminated sites in major cities, creating risks for both human health and environmental quality. The revitalization and redevelopment of these areas have become not only a legal requirement but also a necessity, given the lack of space available for new development in densely packed cities. In São Paulo, for example, the number of restored contaminated sites saw a 23% increase in 2018 compared to the previous year [3]. Despite these efforts, many contaminated areas have since changed their function, with new industrial or commercial activities taking place during environmental assessments. This adds a layer of complexity to the remediation process, requiring detailed analyses to ensure effective cleanup and restoration of the affected sites.

The understanding of contaminant behaviour in the subsurface is directly linked to the characterization of the stratigraphic and hydrogeological context of the site. The velocity and direction of pollutant flow are primarily determined by hydraulic conductivity, groundwater level, and lithological characteristics. In traditional geotechnical and environmental studies, a detailed subsurface investigation involves obtaining a large number of samples, thereby increasing project costs. In the case of contaminations caused by dense non-aqueous phase liquids (DNAPL), such as creosote, improper handling can lead to a preferential flow path carrying pollutants to greater depths. Thus, the combined use of invasive and non-invasive field techniques to support the geological, hydrogeological, and environmental characterization of the study area presents an interesting alternative for obtaining a large volume of information at a low cost and with lower technological risk [4–7]. Electrical resistivity methods are highly sensitive to variations in the soil's physical parameters, primarily influenced by the mineralogical and textural characteristics of the soil. By identifying anomalous values, it is possible to infer the presence of exogenous chemical compounds in soil and groundwater [8, 9]. For this reason, electrical geophysical methods play a significant role in investigating contaminated sites, assisting in delineating the dimensions and behaviour of contamination plumes [10–15]. Several studies have indicated that recent hydrocarbon contaminations result in resistive anomalies [16–18]. However, aged contaminations tend to alter the electrical behavior of pollutants, generating conductive anomalies due to the biodegradation process in the subsurface [19–21]. Studies have revealed that the biodegradation process occurs in both aromatic and aliphatic hydrocarbons, indicating that even complex multi-component pollutants like creosote, with recalcitrant and biocidal substances, are susceptible to natural biodegradation processes by indigenous microorganisms [22–25].

Contaminated sites in urban areas usually have a chemical composition that triggers a series of physical, chemical and biological processes that are distinct from natural soil processes. Therefore, understanding natural attenuation processes in tropical environments remains a challenge, as does understanding how biogeochemical processes can affect and modify natural soil characteristics. Hydrocarbon contamination induces rapid geochemical changes in groundwater, driven by microorganisms and by reactions between contaminants and electron-accepting inorganic substances. These changes occur mainly through specific pathways such as aerobic respiration, denitrification, iron (III) reduction, sulphate reduction and methanogenesis. These processes together lead to the generation of unique biogeochemical signatures [26]. As a result, they contribute to the chemical weathering of grains, causing differentiation in the natural characteristics of the soil, including mineralogical and electrochemical changes, as well as biogeochemical and geobotanical anomalies. They result in an increase in total dissolved solids concentration and, consequently, of the electrical conductivity of the environment [27–29]. However, there is a scarcity of studies

providing field data on the natural attenuation of creosote in tropical environments, posing a challenge to understanding the behaviour of contaminants and how biogeochemical processes can influence and alter the natural characteristics of tropical soils. The present study shows the results of environmental investigations developed in a former creosote wood treatment plant, which operated near one of the main rivers of the city of São Paulo. The research aims to apply methods that are not commonly used in contaminated site investigations in tropical areas, assessing the applicability of non-invasive gamma-ray logging methods associated with electrical conductivity profiling for the stratigraphic characterization of a complex hydrogeological environment. The study attempted to verify the relationship between variations in the physicochemical parameters of the environment and the occurrence of biogeochemical natural attenuation processes of contamination by aliphatic and aromatic hydrocarbons. The biogeochemical natural attenuation processes of contamination by aliphatic and aromatic hydrocarbons were confirmed through chemical analyses of groundwater, biological activity assessing the degradation of the contaminant, and metagenomic classification using a soil sample from the study area.

2 Area location and history of use

The research site is situated in the Jaguaré neighborhood, located in the western part of São Paulo city, Brazil, in close proximity to the University of São Paulo. This area's historical significance is intertwined with the industrialization of the city, having been originally designed as an industrial zone. By 1935, oil storage facilities had already been established by some industries in this region. However, the neighborhood's industrial development saw a marked increase in the 1950s, spurred by the growth of sectors such as construction, textiles, food production, along with chemicals, electronics, and paper manufacturing [30]. The data discussed in this paper stem from the remediation efforts of the former wood treatment facility in Jaguaré (UTM Jaguaré), conducted by the Institute of Technological Research of São Paulo. Between the 1970s and 1990s, this site was utilized as a research and development hub for wood treatment, specifically for applications in the aeronautics industry, as well as for furniture, construction, and railroad ties. The site's operations encompassed all stages of wood treatment, including cutting, chemical preservation, and storage. These processes carried the potential for environmental contamination, given the involvement of various chemicals, such as sodium pentachlorophenol, chromated copper arsenate (CCA), and polycyclic/aromatic hydrocarbons, particularly if proper environmental controls were not in place. All industrial activities at the facility ceased in 2005, with the removal of equipment, and an environmental contamination investigation began in 2011 (Fig. 1).

One of the most problematic chemicals historically utilized in wood preservation is creosote oil. This organic contaminant was extensively employed during the twentieth century as a biocide to preserve wooden railroad ties [31]. At the research site, creosote oil, along with other chemicals, was applied to treated wood and stored in overhead tanks. Over time, poor maintenance of these tanks led to pollutant leaks, resulting in soil and groundwater contamination. Environmental assessments [32] revealed the presence of pollutants such as polycyclic aromatic hydrocarbons, total petroleum hydrocarbons, and various metals in both soil samples (indicating high NAPL saturation) and groundwater samples (dissolved phase), with concentrations exceeding Brazil's regulatory thresholds [33]. This led to the site's classification as contaminated. Given the complexity of contaminant migration through subsurface layers, a thorough stratigraphic analysis is essential to comprehending contaminant flux behavior and developing effective remediation strategies. An additional complicating factor is the site's proximity to major drainage systems in São Paulo, including the Jaguaré Stream and the Pinheiros River [34]. The occurrence of contaminated sites near primary drainage networks is a frequent issue in densely populated metropolitan areas.

3 Geological-geotechnical context of the study area

The city of São Paulo is situated in the geological context of the Paraná Sedimentary Basin, a large intracratonic basin in the central-south portion of the South American Platform [36]. The sedimentary basin is one of the most important sedimentary basins in South America, as it contains significant deposits of natural resources such as petroleum, natural gas, coal, and groundwater [37, 38]. The water resources originating from this basin are essential for supplying cities, industries, and agriculture throughout South America and need to be monitored and preserved [39]. The geological mapping of the city of São Paulo is characterized by the Precambrian basement, approximately 600 million years old, composed of magmatic and metamorphic units, and tertiary sediments of the São Paulo Basin, essentially composed of

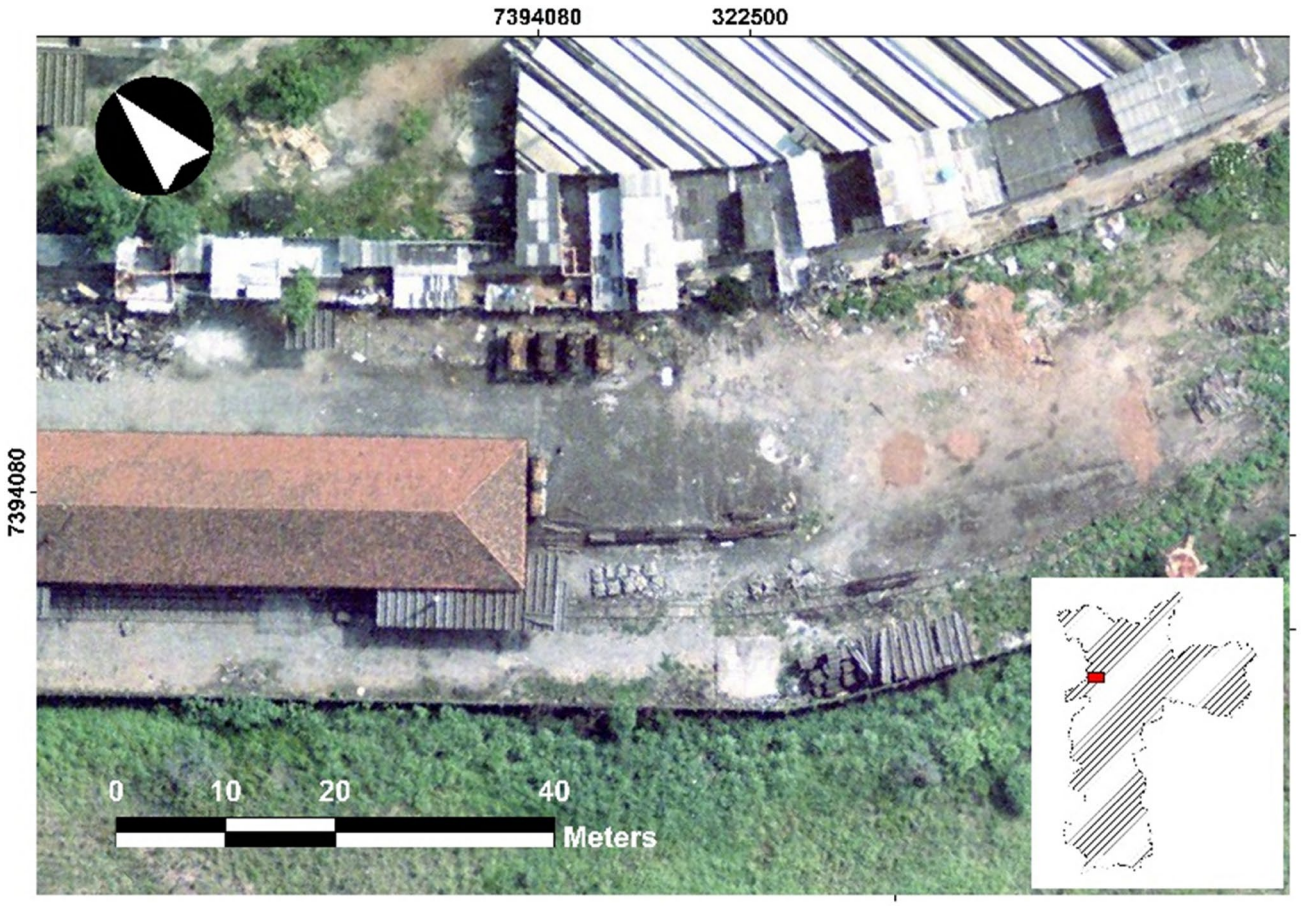

Fig. 1 Aerial image of the study area in 2004 [35], with evidence of the presence of aerial tanks for chemical products storage, the autoclave supply operation track, and residual contamination by creosote on the surface

sedimentary rocks of different grain sizes, conglomerates, and mudstones. Overlying these formations, Quaternary covers composed of sands, clays, and conglomerates are observed, resulting from the action of rivers, lakes, and oceans that existed in the area during past geological periods [40] (Fig. 2). The interaction between sedimentary and igneous rock formations plays a fundamental role in the geology of the city, influencing aspects such as topography, water resources, and geotechnical challenges faced in urban development.

The study area is located in the region of the Pinheiros River floodplain and, as a result, exhibits a typical floodplain stratigraphy, made up of layers of clay, sand and gravel, resulting from the frequent flooding of the river during flood periods [6]. These deposits overlie the Tertiary sediments of the Itaquaquecetuba Formation [38]. Important geological studies have been carried out in the vicinity of the study area as part of the effort to geologically map the University of São Paulo campus. For example, [39] carried out geological mapping from an excavation parallel to the Pinheiros River, while other studies [37, 40] focused on detailed characterization of the alluvial deposits and analysis of the geotechnical conditions of the region. In this study, lithotypes from the Itaquaquecetuba Formation were observed (Fig. 3). This geological formation exhibits typical characteristics of an interwoven river deposit system and typically comprises five lithofacies: medium to coarse-grained sandstones, conglomerates, massive medium to fine-grained sandstones, massive mudstones, sandy siltstones, and sub-angular blocks of basement rocks. The local geological characterization revealed that changes in flooding conditions, currents, and sediment transport, over time, resulted in a significant variation in the arrangement of sediment layers, making it challenging to identify and characterise the layers in detail. The composition of sediments can vary significantly on small scales, making it difficult to collect representative samples and extrapolate results to a larger area, a procedure typically carried out in geo-environmental studies [39]. Therefore, the stratigraphic context is a relevant and interesting factor in this study to understand the behaviour of contaminants in the physical environment since the heterogeneity of stratigraphic layers, such as the presence of clay lenses, will influence the speed of contaminant percolation in the physical environment, for example.

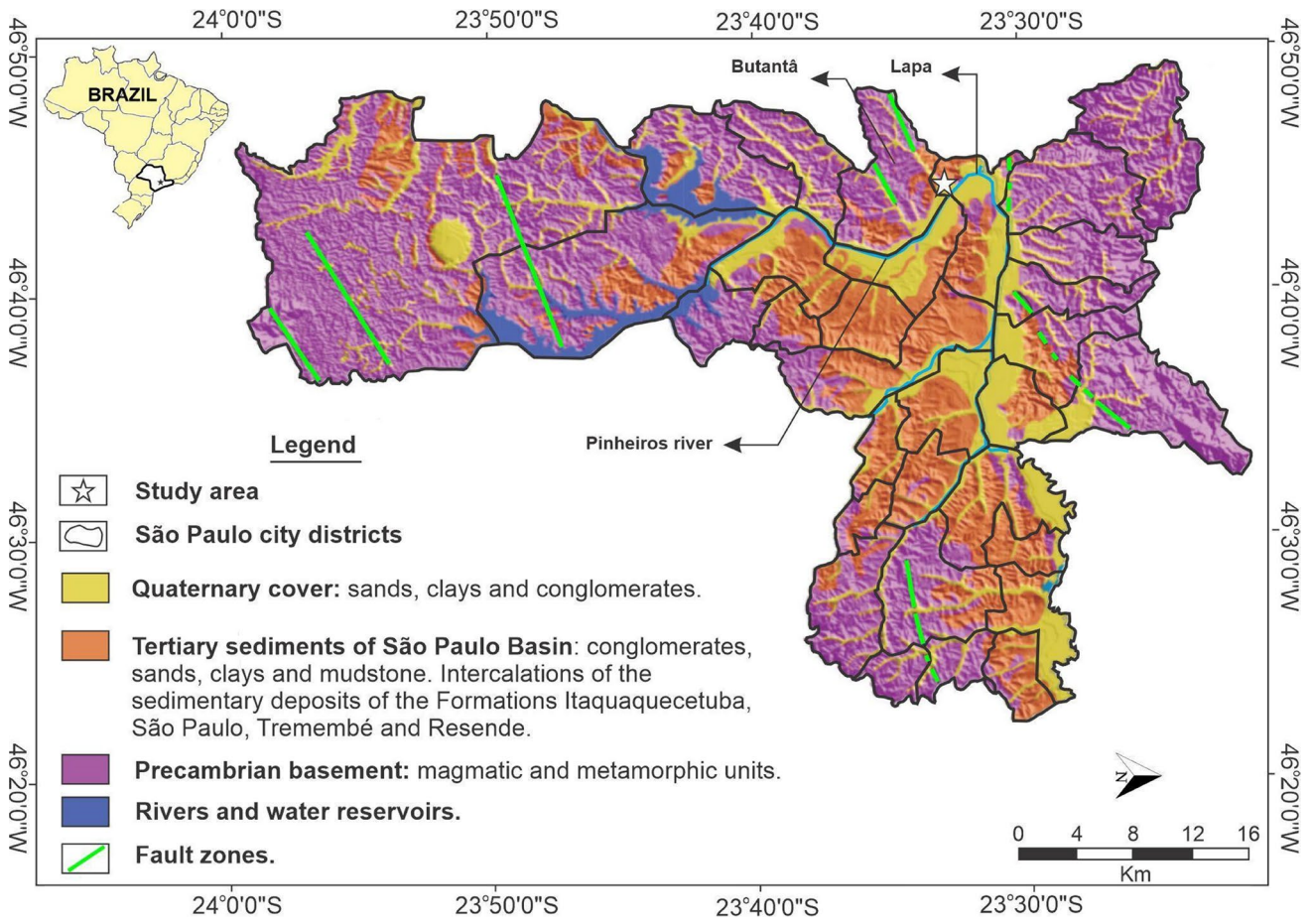

Fig. 2 Geological context of the city of São Paulo and the location of the study area [modified from [37]]

4 Materials and methods

This study employed a combination of high-resolution site characterization (HRSC) methods, including techniques like gamma-ray logging and electrical conductivity profiling, drone imagery, and groundwater chemical analyses. These approaches were integrated to generate a comprehensive characterization of the site, revealing signs of natural attenuation of the creosote contamination. The results from the HRSC techniques were corroborated by particle size distribution analyses conducted on soil samples taken from the study area. Additionally, groundwater samples from monitoring wells were analyzed for total petroleum hydrocarbons (TPH), polycyclic aromatic hydrocarbons (PAH), electron acceptors, and metabolic byproducts. These assessments were carried out along two transects (Transects 1 and 2 in Fig. 4) that aligned with the groundwater flow, ensuring a detailed understanding of the subsurface contaminant dynamics. The high-resolution aerial photogrammetric survey was executed with the use of a small drone, with high spatial resolution, and subsequent image processing. The drone flight reached 120 m from the horizontal plane of reference, with a resolution of 4.65 cm/pixel, surveying an area of 79 ha. The aerial images were processed in ESRI® ArcMap 10.6.0 and projected in the UTM coordinate system in DATUM Sirgas 2000, generating an orthophoto, that allowed detailed visualization of the current situation of the study area. Figure 4 illustrates the location of the high-resolution site characterization investigations, groundwater sampling, and geological surveys developed on the site. The high-resolution site characterization methods used were the natural gamma profiling performed in the groundwater monitoring wells, and the electrical conductivity profiling (EC), with electrical conductivity sensors in a dipole-type array with horizontal alignment, chosen due to the large application of this technique in the investigation of contaminated sites, as it allows the correlation of the measured values with analytic data.

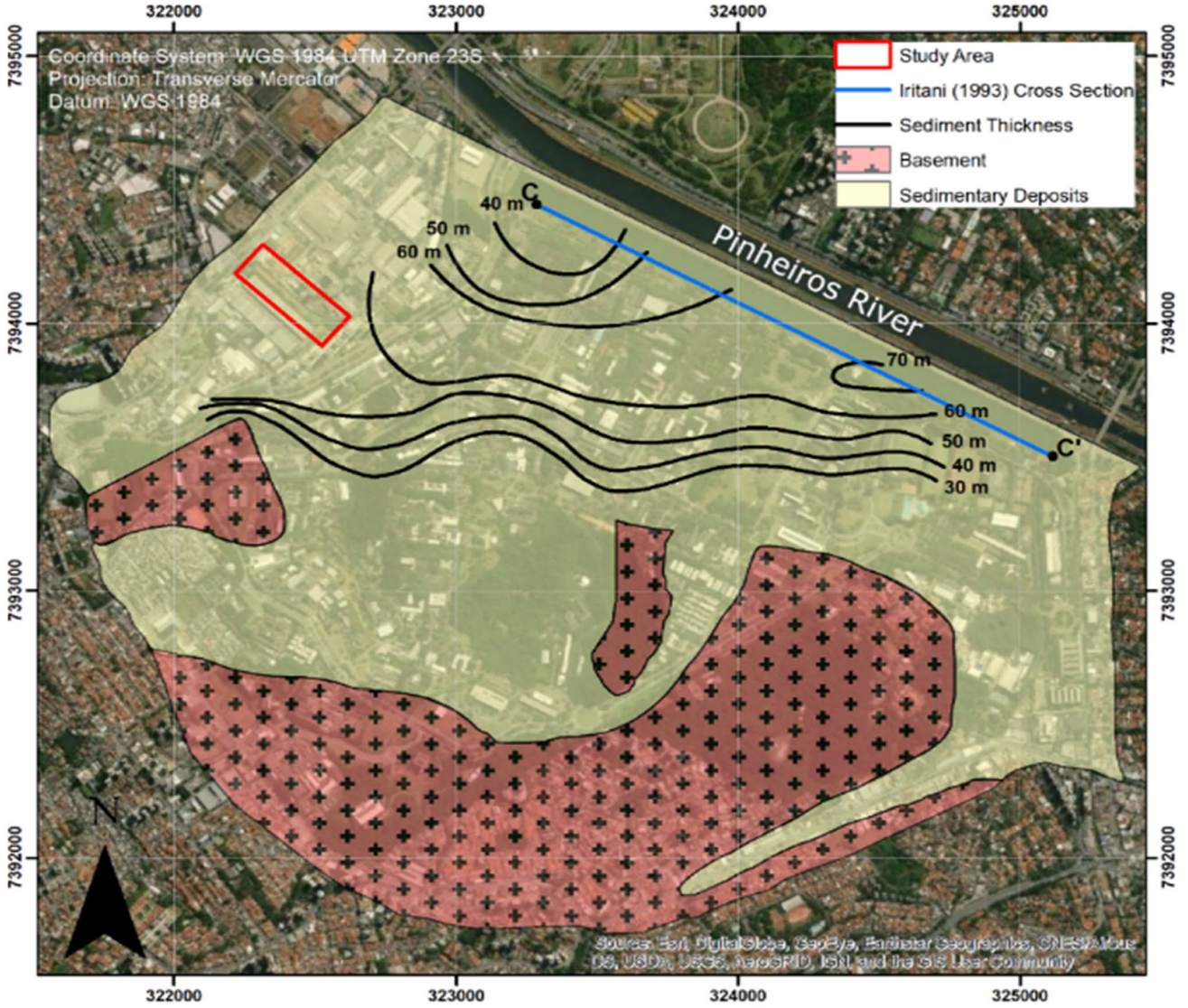

Fig. 3 Geological map of the University of São Paulo based on previous studies. Study area was delimited in red [modified from [39]]

4.1 Laboratory tests—soil characterization

In order to assess the stratigraphic variation along the soil profile within the study area, soil samples were taken at the SOIL-01 location for laboratory-based physical analysis. The samples were obtained through the direct push method [41], utilizing a pneumatic hammer, polyvinyl chloride (PVC) samplers, and jacketed rods of 140 cm, with a maximum sampling depth reaching 750 cm. Prior to sampling, the soil texture was estimated manually [42], and samples were gathered at each point of stratigraphic change, resulting in 17 samples that were subsequently analyzed for particle size distribution. For particle size analysis, sedimentation was employed to assess the fine fraction of the soil, while sieving was used to categorize the coarser fractions. Based on the particle size distribution, soil particles were classified into seven distinct categories, following the [43]: clay (< 0.002 mm), silt (0.002–0.06 mm), fine sand (0.06–0.2 mm), medium sand (0.2–0.6 mm), coarse sand (0.6–2.0 mm), and particles larger than 2 mm. This approach aimed to provide a detailed understanding of subsurface textures, confirming the visual and tactile descriptions, and aiding in the identification and differentiation of the stratigraphic layers.

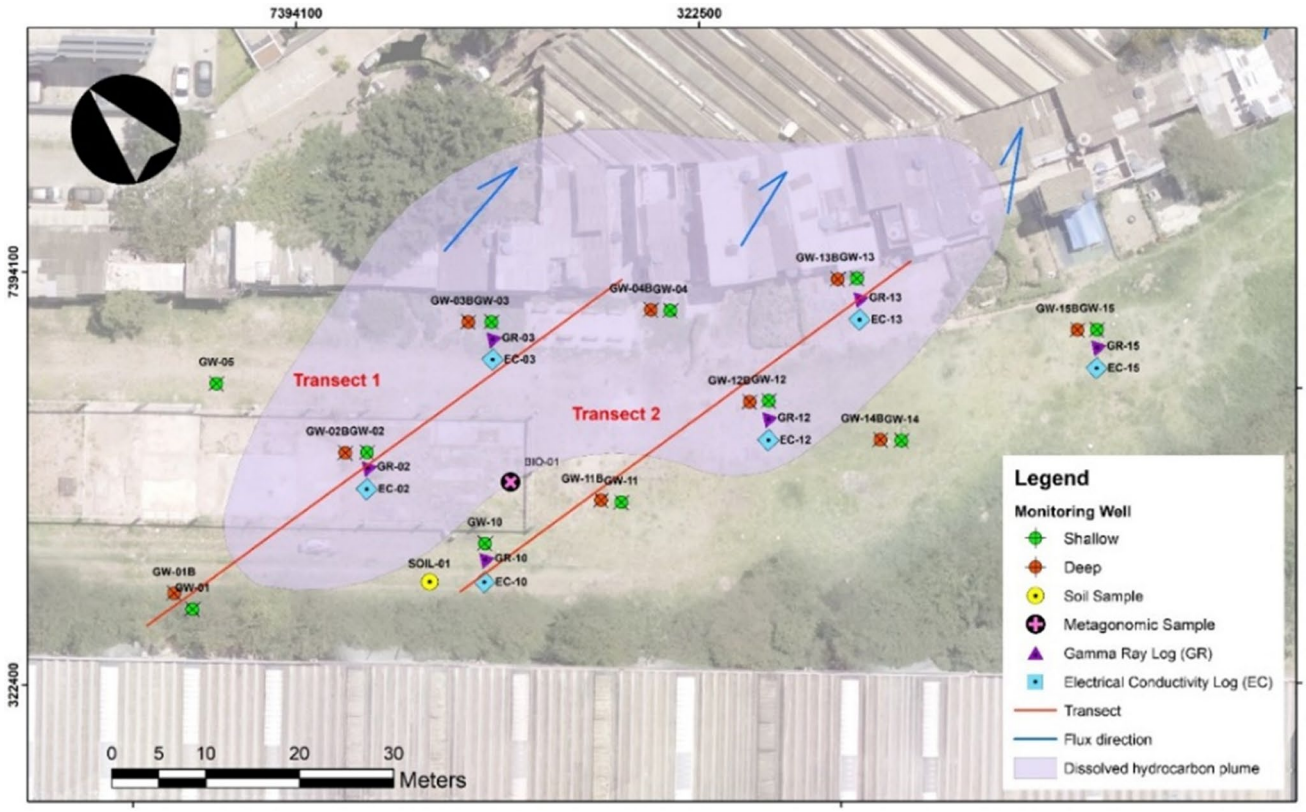

Fig. 4 Scheme of data acquisitions performed in the study area, detailing the locations of investigation and monitoring test points, the two transects used, and the flow direction

4.2 Electrical conductivity profiling (EC)

Techniques based on soil drilling principles, commonly referred to as penetrometric methods, are widely employed in geoenvironmental investigations. These approaches facilitate the measurement and recording of various data types—geotechnical, geophysical, hydrogeological, and analytical—along profiles or cross-sections. One of the key features of penetrometer systems used in high-resolution geoenvironmental research is the integration of sensors that can measure the electrical conductivity of subsurface materials. The technique discussed by [44] enables detailed soil profiling through percussive driving, capturing continuous electrical conductivity measurements at centimeter-scale intervals, offering a high level of precision [45]. A notable advantage of this method is its ability to correlate data with other investigative techniques, such as gamma logging and seismic testing, as demonstrated in this study. In rocks and soils, electrical current is transmitted by two primary mechanisms: electronic conduction, through the solid rock matrix, and ionic conduction, facilitated by ions present in the pore water. These processes differ between the vadose zone—where the properties of the soil matrix, including granulometry and mineral composition, dominate—and the saturated zone, where the characteristics of the liquid phase play a more critical role in electrical conductivity [46]. Of the two, ionic conduction is typically the most significant mechanism in electrical resistivity surveys [47]. Among the various physical properties of rocks and minerals, electrical resistivity demonstrates the greatest variation range, making it an invaluable tool for assessing contaminated sites. Contaminants often alter the natural properties of their environment, leading to detectable changes in electrical resistivity, as captured by geophysical methods [48]. Furthermore, the identification of small-scale stratigraphic changes is essential, as these can substantially affect the movement of groundwater and solutes within the subsurface. However, few subsurface characterization methods provide sufficient detail on hydrostratigraphy. Electrical conductivity variations in soils and rocks also correspond to lithological changes, making conductivity sensors particularly useful for evaluating stratigraphic differences throughout a soil profile [49].

In this study, six sets of electrical logging measurements were performed using a Geoprobe® 6620DT direct push system and the MH6534 probe (Fig. 5A). The probe's electrical conductivity (EC) sensor is a device used to measure

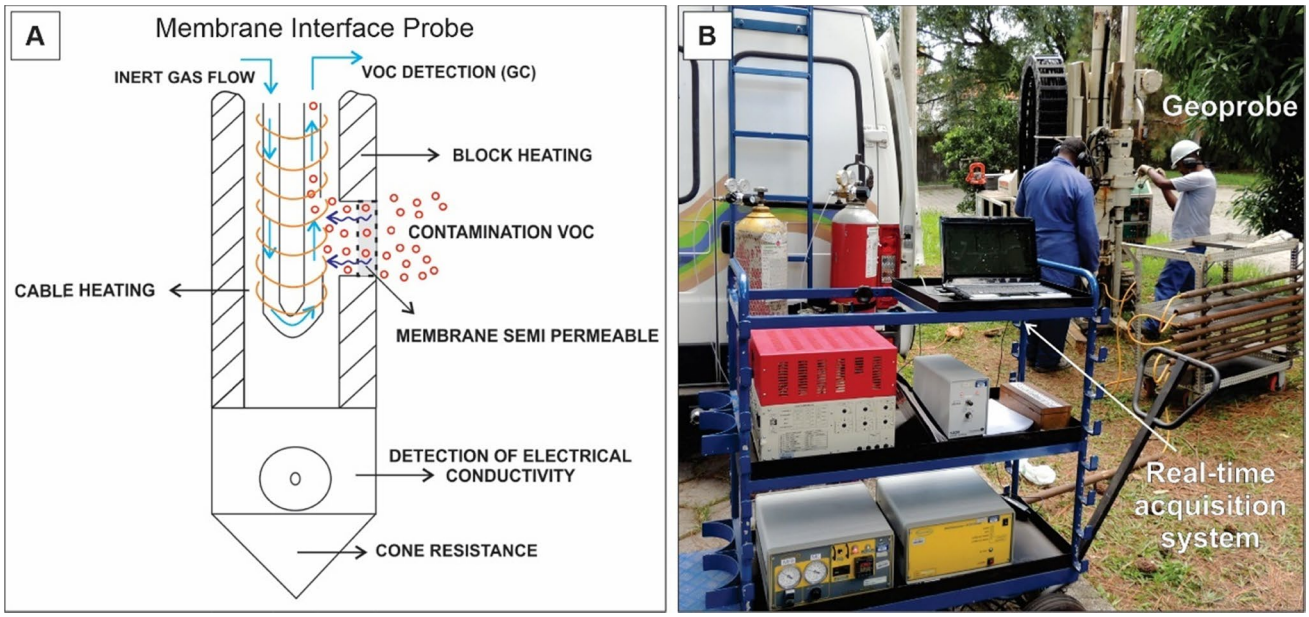

Fig. 5 **A** Schematic of the Membrane Interface Probe elements (detail of the CE sensor on the tip). **B** Field drilling (detail of Geoprobe and real-time acquisition system)

the electrical conductivity of soil and groundwater in situ. Electrical conductivity is a physical property that indicates a material's ability to conduct an electric current and is directly influenced by the presence of dissolved salts, conductive minerals, humidity and temperature. The Geoprobe® MH6534 sensor operates on the principle of electromagnetic induction. The system consists of two sets of coils: an emitting coil and a receiving coil. The emitting coil generates an alternating electromagnetic field that induces electrical currents in the surrounding soil. These currents in turn generate a secondary magnetic field which is detected by the receiving coil. The strength of the secondary magnetic field is directly related to the electrical conductivity of the material surrounding the probe. The EC sensor is a dipole-type array. This type of array is particularly sensitive to variations in electrical conductivity along horizontal layers, which is essential in detailed stratigraphic characterization studies in contaminated areas. The main advantage of the horizontal array is its ability to detect subtle changes in conductivity along the interfaces between different soil layers in real time (Fig. 5B), such as those between clay and sand or between contaminated and uncontaminated sediments. This is because the horizontal orientation maximizes the conductivity response along the plane of the layer, making it more effective than vertical or coaxial arrangements in capturing conductivity variations parallel to the soil surface.

The drilling site was prepared by stripping away the top 50 cm of surface gravel to prevent potential damage to the equipment. This was followed by conducting initial and final response tests to ensure that the response standards were met and the quality of the results was maintained. Subsequently, the acquired data were analyzed in conjunction with laboratory soil texture analyses to investigate how electrical variations correlated with clay content in the soil.

4.3 Natural gamma logging

The geophysical technique utilized in this study was gamma well logging, where the primary measured property is the gamma radiation emitted naturally by the geological formations encountered during drilling. The radioactivity of these formations is primarily influenced by three elements: potassium (K), uranium (U), and thorium (Th), with variations in radiation levels indicating different lithologies—higher levels typically associated with pure clay deposits and lower levels linked to sandy formations. Well logging involves capturing vertical profiles that provide continuous data on a specific physical property of the medium within wells or boreholes. The measurements typically extend only a few tens of centimeters into the surrounding formation, focusing on the area immediately adjacent to the well. The gamma probe used in this study can function effectively in both cased and uncased holes, regardless of the groundwater level. For this research, gamma logging was conducted in six wells situated in the study area, employing a gamma probe logging system developed by Robertson Geologging® and equipped with a high-sensitivity NaI

crystal. The probe was lowered into the boreholes at a speed not exceeding 4 m/min. The main aim of this method is to achieve lithological characterization and recognition, facilitating stratigraphic correlation between the wells and with tests that evaluate other physical parameters, as outlined in this study [50, 51].

Spectral gamma-ray logs record the relative contribution of the natural radioactivity in a sedimentary succession and stratigraphic characterization. According to [52] in siliciclastic sedimentary rocks, K is concentrated in micas, micaceous clays, and sodium and potassium feldspars; Th occurs in sand and silt-sized grains of certain heavy minerals and U accumulates in phosphates, organic matter, and uranium-bearing minerals. [53] describe the use of spectral gamma-ray logs in testing and refining high-resolution stratigraphy in fluvial strata; however, [54], when studying the concentrations of uranium, thorium, and potassium, observed their presence in different formations, indicating that the radioactive source is associated with different compositions, and their respective concentrations depend on the depositional environment. [55] successfully employed gamma logging as a High-Resolution Site Characterization (HRSC) technique to distinguish between higher clayey layers (characterized by low permeability) and sandy layers (permeable) in a contaminated area affected by hexavalent chromium (Cr VI), demonstrating the efficiency of applying gamma-ray to the characterization of stratigraphy in contaminated sites. The tests were carried out in the following groundwater monitoring wells installed in the study area: GW-02 (6.0 m), GW-03 (6.35 m), GW-10 (7.50 m), GW-12 (7.0 m), GW-13 (6.0 m), and GW-15 (7.9 m), aiming to apply the concept of alignment in two transects, to observe the behavior of gamma-ray values in the subsurface as a function of the presence of hydrocarbon contamination in the groundwater.

4.4 Groundwater contamination, geochemical and biological monitoring

The evaluation of the existence of biogeochemical processes of natural attenuation was carried out in the existing groundwater monitoring wells in the study area, each monitoring cluster being composed of wells installed in two depth levels: Shallow—between 6.0 to 8.2 m bgl (below ground level), and Deep—between 10.6 to 12 m bgl. The clusters were arranged to include one monitoring well located upgradient of the contaminant spill, one within the NAPL source area, and two directly downgradient of the source area, within the dissolved contaminant plume. Transect 1 also included one well downgradient of the contamination source, but laterally offset from the direction of groundwater flow (GW-5), and in transect 2 two more clusters were added (GW-14 and GW-15). The identification of electron acceptors available in an aquifer is critical to evidence the occurrence of microbial and geochemical processes in the area. Thus, the study included the analysis of sulfate (SO_4^{2-}) and nitrate (NO_3^-), using the [56], and dissolved oxygen (DO), analyzed in flow through-cell during pumping on site [57]. Iron concentration is an indicator of anaerobic degradation routes of organic carbon via Fe^{3+} reduction, and methane is an indicator of methanogenesis processes during the biodegradation of petroleum hydrocarbons. Thus, their presence is also an indicator of the existence of metabolic by-products. Iron (Fe^{2+}) was analyzed by the [58], and methane (CH_4) by the [59]. The contaminants evaluated were total petroleum hydrocarbons (results reported as ΣTPH), analyzed by the [60], and the 16 USEPA priority polycyclic aromatic hydrocarbons (results reported as ΣPAH_{16}), analyzed by the [61]. The presence of polycyclic aromatic hydrocarbon-degrading biological activity and metagenomic classification was carried out through the collection of a sample (BIO01) in Unit 3 (5 m bgl) in the saturated zone. PCR assays and determination of polycyclic aromatic hydrocarbon concentrations were conducted [62]. The extracted DNAs were subjected to the amplification reaction flanking the conserved region of 16S rDNA, and the primers used were 16S Illumina F and 16S Illumina R [63]. The sequencing and classification of the amplified DNA with primers for the 16S gene (amplicon) were sent to the laboratory for sequencing of fragments of 150–250 bp in both directions with a coverage of 100,000 paired-end reads. The raw data generated were downloaded and stored for processing and analysis. Sequencing was performed on a MiSeq system (Illumina, San Diego, CA, USA), with taxonomic identification using the SILVA 138 database [64].

5 Results

The analysis of the study area involved utilizing geophysical and geoenvironmental techniques. Consequently, the results from the methods employed are initially outlined separately, followed by a synthesis of the interpretations regarding the observed physical properties.

5.1 Stratigraphic characterization of the site

Based on the results from the visual-manual analysis of the collected soil samples, the background soil profile of the area was categorized into four units and a lens. These units were differentiated into strata according to their formation characteristics, with detailed descriptions provided in Fig. 6. The pedogenetic processes observed throughout the soil profile are influenced by factors such as the material of formation, deposition, position within the subsurface, and groundwater level, which are primarily linked to fluvial depositions in the region of the former floodplain of the Pinheiros River, within the São Paulo Sedimentary Basin. As noted by [65], these depositions exhibit basal layers of gravel and cobble, fine to coarse sands in intermediate portions, and peaty layers at the surface (organic clays). Above these sediments lie technogenic deposits that create landfill layers of 2 m or more, overlaid on the original floodplain [65]. This observation aligns with the soil profile identified in the area, characteristic of zones influenced by the fluvial material of the Pinheiros River.

According to the classification provided by the World Reference Base for Soil Resources [66], the soil in the study area is identified as an Epileptic Humic Technosol. This type of soil is characterized by properties and pedogenesis significantly influenced by human activities, as evidenced by the presence of technological materials located less than 100 cm from the surface. Additionally, there is a layer of humic matter containing more than 1% of organic carbon situated beyond 50 cm of the mineral soil surface. The presence of external materials and the modifications observed in the area, such as cobblestones and gravel in the upper layers of the profile, as well as the identified landfill layer, greatly affect the soil characteristics. According to [40], the occurrence of organic clays is typical of alluvial deposits found in Quaternary sediments within the metropolitan region of São Paulo, suggesting a historical groundwater level that was higher than present conditions.

The results from the soil granulometric analysis (Table 1) support the observations made during the visual-manual assessment, revealing that the laboratory classifications provided a more precise understanding than field descriptions. The data indicate that units 01 and 02 exhibit high clay content, which decreases significantly beyond 3.4 m, where sand particles become predominant. This is particularly relevant for the vertical spread of contaminants, especially in areas containing dense nonaqueous phase liquids (DNAPLs), as the pore distribution characteristics can greatly influence the movement of contaminants throughout the stratigraphic profile. Notable increases in clay content are observed in three samples: from 3.87 to 4.15 m, from 5.8 to 6.0 m, and from 7.05 to 7.10 m. These deposits are representative of alluvial deposits. The abrupt texture transition layers impact the rate of vertical hydraulic conductivity, primarily affecting the vadose zone and percolation processes, leading to preferential horizontal flow. Thus, identifying these layers is critical

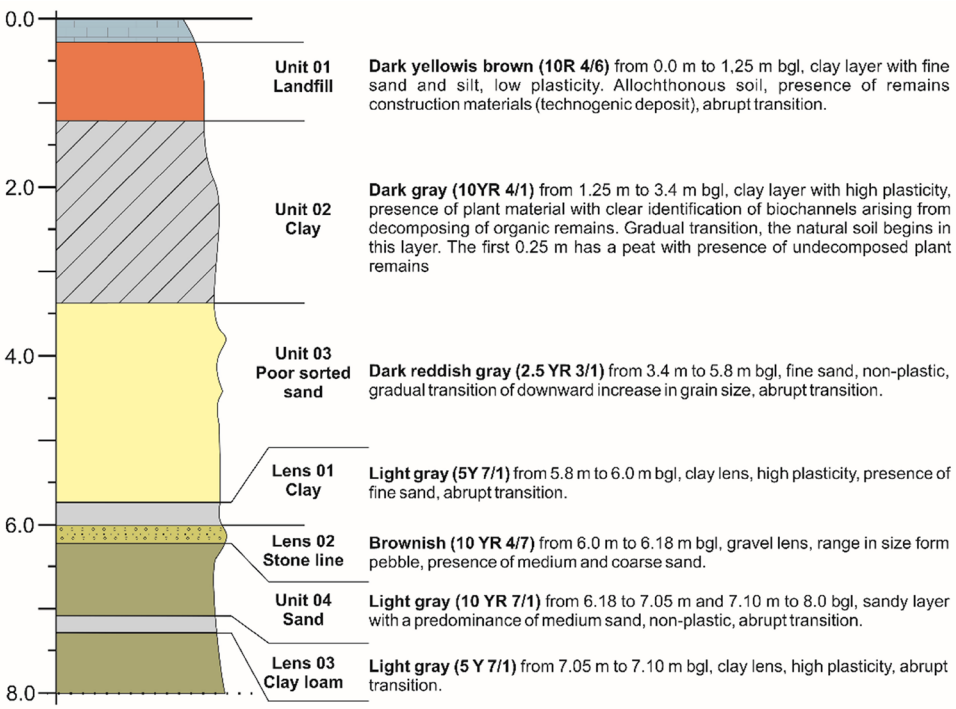

Fig. 6 Description of the stratigraphic profile in the study area (units and lens)

Table 1 Results of the particle size analysis

Lithology	Top	Base	Clay	Silt	Sand			> 2 mm
					Fine	Medium	Coarse	
	(m)		(%)					
Unit 01 Landfill	0.25	1.25	55.2	3.2	25.5	11.4	4.7	0.0
Unit 02 Clay	1.25	1.50	-	-	-	-	-	-
	1.50	3.40	73.0	18.3	8.1	0.4	0.2	0.0
Unit 03 Poorly sorted sand	3.40	3.87	6.5	19.5	67.4	6.5	0.1	0.0
	3.87	4.15	23.0	42.0	34.0	1.0	0.0	0.0
	4.15	4.40	0.0	2.0	76.0	18.0	1.0	3.0
	4.40	4.90	0.0	0.0	16.0	56.0	26.0	2.0
	4.90	5.00	6.0	20.0	60.0	12.0	2.0	0.0
	5.00	5.27	0.0	23.0	62.0	13.0	2.0	0.0
	5.27	5.40	8.0	16.0	56.0	17.0	30	0.0
	5.40	5.68	5.0	2.0	14.0	56.0	22.0	1.0
	5.68	5.80	0.0	0.0	16.0	58.0	24.0	2.0
Lens 01 Clay	5.80	6.00	57.0	14.0	13.0	7.0	4.0	5.1
Lens 02 Stone line	6.00	6.18	0.0	1.4	7.4	10.5	23.5	58.2
Unit 04 Sand	6.18	7.05	3.0	2.0	8.0	44.0	41.0	2.0
Lens 03 Clay loam	7.05	7.10	39.4	34.5	9.3	10.5	6.3	0.0
Unit 04 Sand	7.16	8.0	0.0	2.0	4.5	18.3	71.7	3.5

since clay layers within the subsurface can serve as natural barriers to vertical flow. Between 6.00 and 6.18 m, a layer of cobbles was detected, with 58.2% of the materials exceeding 2 mm in diameter. This layer is characteristic of the Holocene deposits from the alluvial plain of the Pinheiros River (Stone Lines), as noted by [36], where such deposits are located at the base of alluvium in floodplain regions and low terraces, comprised of sandy and clay layers rich in organic matter.

5.2 Electrical conductivity log (EC)

The profiling results for electrical conductivity were obtained at intervals of 1.6 cm, recording minor changes and discretization along the measurement profile. This investigation technique allows for the identification of different lithologies, as higher electrical conductivity values typically correlate with higher clay content, whereas lower conductivity values are indicative of sandy materials. The behavior of the profiling indicates that electrical signal variations adhere to a consistent pattern, despite the spatial differences in drilling locations. Clay layers exhibited electrical conductivity values exceeding 20 mS/m, while sand layers displayed values below 15 mS/m. Notably, two peaks in conductivity values were recorded at depths of 6 m and 7.2 m, likely linked to the presence of clay lenses beneath the surface. This discretization aligns with findings from [44], who reported that the dipole array exhibits increased sensitivity in detecting small environmental variations, although it is also more prone to contact issues with the profiling walls due to its configuration of just two horizontally arranged electrodes.

The profiling results reveal a correlation between electrical conductivity responses and particle size data. The highest field-recorded conductivity values are associated with clay-rich layers present at shallow depths in the profile. As noted by [67], variations in soil texture can produce intricate spatial patterns in electrical conductivity readings, significantly influenced by changes in soil texture, moisture content, and salinity. Therefore, despite utilizing indirect measurement techniques, it remains essential to conduct sampling for the validation and calibration of the interpretations. In this study area, the implementation of electrical conductivity profiling emerged as a rapid and precise approach for acquiring indirect data regarding stratigraphic distribution. Although the area exhibits

significant vertical stratigraphic variation with thin layers, this technique successfully characterized and identified these layers. Throughout the profiles, the electrodes detected narrow electrical anomalies that correspond to granulometric variations identified as clay layers in Unit 01 (0.26 to 1.25 m) and sand layers in Unit 03 (6.0 to 8 m). These findings underscore the material's heterogeneity within the profile being assessed. The dipole array was also capable of pinpointing clay lenses with thicknesses ranging from 5 to 13 cm, as noted during the visual-manual description. This outcome highlights the effectiveness of the electrical conductivity sensors and the array system in acquiring stratigraphic data for thin layers.

5.3 Gamma Ray Log (GR)

The results of gamma well logging is presented in Table 2 and graphs (profiles) that show the variation of the gamma-ray emission count (in units of cps—counts per second) as a function of depth of variation of the stratigraphic composition of the subsurface [51]. During the borehole operations conducted in the study for the stratigraphic characterization of the site, the presence of several clay lenses in the unsaturated layer, intercalated with sandier layers, was observed. This stratigraphic behavior marked by the presence of this finer-grained material was expected since the study area is situated in the floodplain region of the Pinheiros River. Therefore, the results of the gamma ray geophysical logging were focused on identifying soil properties at small intervals (centimetres) above the water level. Variations in the grain compositions of soils in the unsaturated zone are directly related to the lateral and vertical extent of creosote development in the study area. The different units determined in the stratigraphic characterization of the area exhibited variations in natural gamma ray counts with depth. Units 1 and 2 had readings with little fluctuation, with values between 100 and 150 cps, which may be related to the presence of lithologies with high clay-mineral contents. However, sandy lithologies with a high concentration of potassium feldspars can also present high values of gamma count, above 150 cps, as observed in GW-02, GW-03 and GW-10 logs close to a depth of 4 m. Although, the values obtained in GW-12, GW-13 e GW-15 logs is a considerable increase in the gamma-ray emission count values for the same depths. The gamma logging data obtained from the investigation of six wells within the study area is shown in Fig. 7.

These peak values observed might indicate the presence of a sandy layer enriched with potassium feldspars or a lithology that contains elevated levels of clay minerals. However, the electrical conductivity values obtained in the electrical conductivity log were below 15 mS/m, consistent with values for sandier lithologies. These values are associated with changes in the characteristic of the material deposited along the fluvial plain of Pinheiros river. As the study area is located in the Itaquaquecetuba formation, its fluvial deposits are composed of part of the fluvial plain of Pinheiros river, which has coarse arcosean sandstones with crossed stratifications and may contain levels of clay-silt and conglomerates with pebbles. Two samples were prepared: Sand A (5.00–5.27 m), and Sand B (5.68–5.80 m), both located in Unit 3 of the SOIL-01 point (background). Using a Leica stereomicroscope (model M165C), the samples were arranged in Petri dishes, which were leveled for a better observation of the distribution of the grains, thus avoiding distortions of the image focus during the acquisition (Fig. 8).

Sand A sample presents a predominance of the fine sand fraction, and a greater abundance of quartz minerals, with the presence of biotite and feldspar. In the Sand B sample, the mineral fraction is larger, between medium and coarse sand fractions, with the presence of biotite and feldspar minerals with a larger diameter. High gamma-ray values are indicators of the presence of feldspar and micas, being associated with arcosian materials and alteration products, such as kaolinite, sericite, and chlorite [68], corroborating with the gamma-ray results and geological description presented by [51, 69].

Table 2 Descriptive statistics for gamma-ray log data

Variable	Mean	Min	Max	SD	Variance
GW-02	126.1	90.7	155.6	16.8	281.5
GW-03	127.0	76.9	188.7	22.9	526.2
GW-10	143.5	82.9	238.4	35.5	1257.3
GW-12	155.1	90.3	287.0	38.4	1474.5
GW-13	134.9	89.6	186.2	17.9	319.5
GW-15	199.9	93.5	541.3	91.6	8393.9

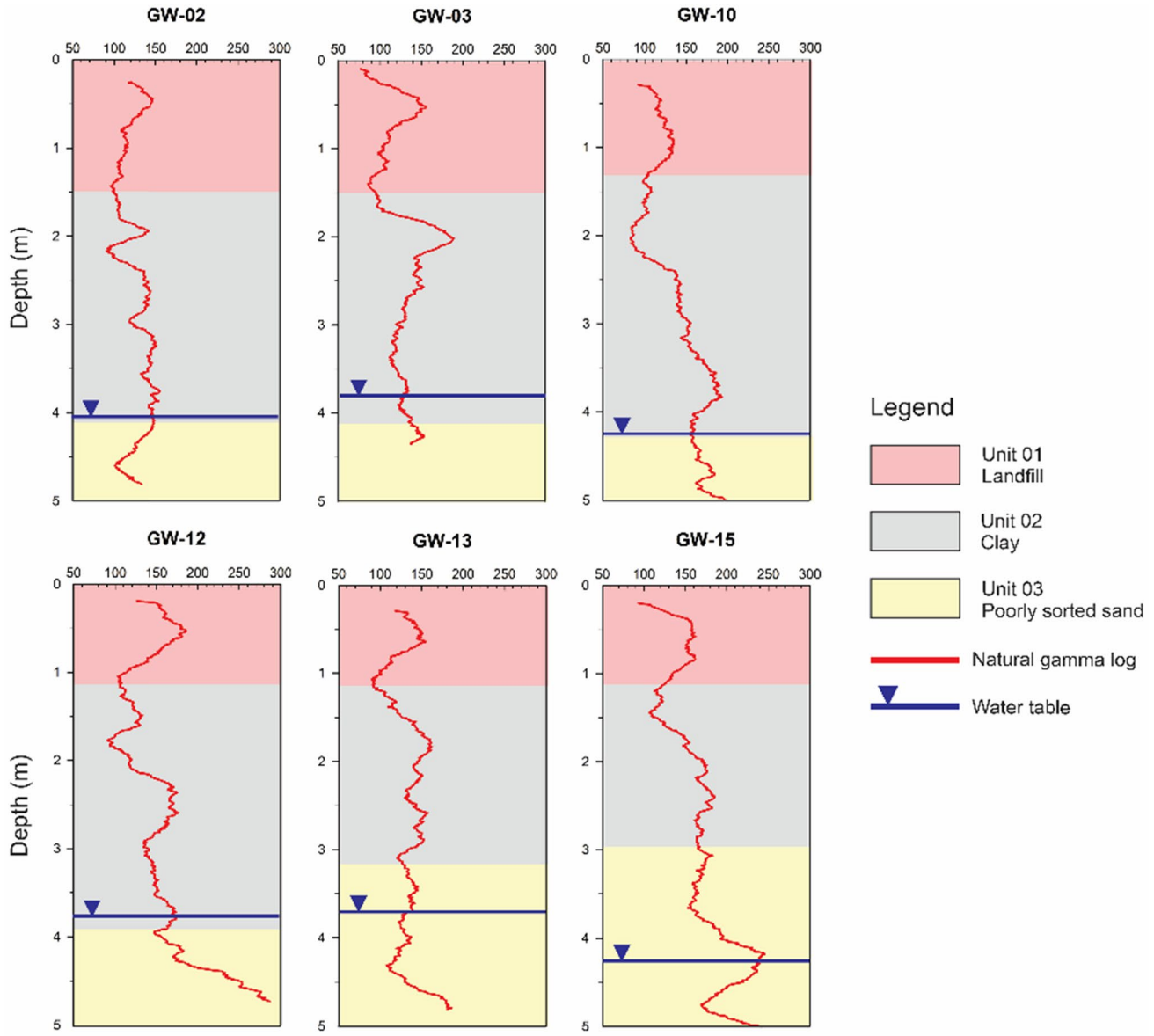

Fig. 7 Results of gamma well logging in the study area

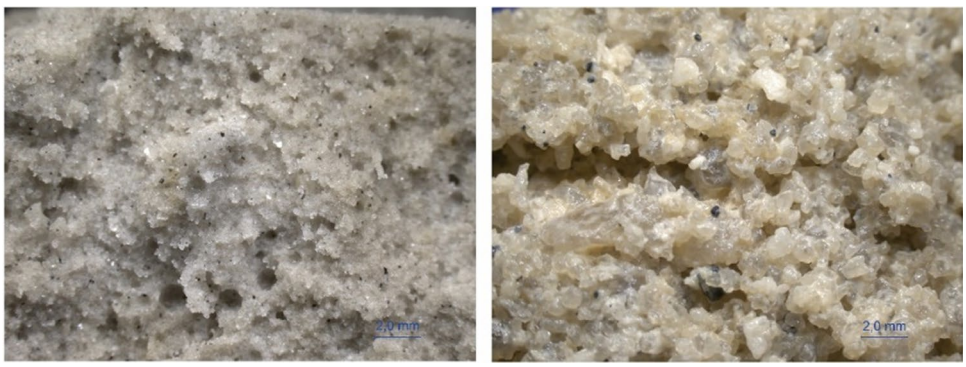

Fig. 8 Image of Unit 3 samples for the depths of 5.00–5.27 m (left), and 5.68–5.80 m (right). It is possible to identify the variation of the material that composes the unit, with its increasing grain size of sand, feldspar mineral, and biotite particles

5.4 Groundwater contamination, geochemical and biological monitoring

The analytical results validated the existence of groundwater contamination resulting from the former operations of UTM Jaguaré, and the sources of contamination were identified in the areas where the monitoring wells GW-02 (ΣPAH = 8.13 mg/L and ΣTPH = 10.74 mg/L), GW-13 (ΣPAH = 15.57 mg/L and ΣTPH = 29.37 mg/L), and GW-13B (ΣPAH = 16.38 mg/L and ΣTPH = 18.09 mg/L) are located. Contamination values of PAH and TPH were observed in GW-03, GW-03B, GW-04, GW-11, and GW-12, classified as zones under the influence of the contamination plumes, due to the presence of concentrations of polycyclic aromatic hydrocarbons and total petroleum hydrocarbons below the reference level (Table 3).

Based on the data obtained, the area of monitoring wells GW-12 and GW-12B was classified as Source 1. This classification was based on knowledge of the physical and chemical characteristics of the contaminant, the origin of the contamination activity and the specific context of its location, as detailed in Sect. 2.2. Although the concentrations of total petroleum hydrocarbons (TPH) and polycyclic aromatic hydrocarbons (PAH) in the GW-12B deep well are low, this area was identified as a primary contamination source due to surface contamination associated with operations in the region, where autoclaves were located (Fig. 9). Operational activities in this area mainly affected the topsoil, and the clay layer identified in Unit 2 acted as a barrier, controlling the vertical percolation of creosote and limiting the migration of contaminants to deeper levels, which explains the low concentrations observed in GW-12B. Therefore, the significant contamination is present in the superficial zone, where the anthropogenic impact was more direct, justifying the classification as Source 1. On the other hand, the area of wells GW-13 and GW-13B was classified as Source 2 due to the presence of contamination at both levels (superficial and deep), with higher concentrations of TPH and PAH, especially at level 1. This extensive and intense contamination is due to the lower density of the hydrocarbons, which allowed for

Table 3 Analytical results for contamination values, electron acceptors, and by-products evaluated in groundwater

	ID of monitoring well	Length (m)	Level Type	Water table (m)	ΣPAH_{16} (mg/L)	ΣTPH (mg/L)	OD (mg/L)	NO_3^- (mg/L)	Fe^{2+} (mg/L)	SO_4^{2-} (mg/L)	CH_4 (mg/L)
Transect 01	GW-01	0.0	Shallow	4.79	0.001	< 0.300	1.1	< 0.50	11.0	37.0	< 0.100
	GW-02	25.0		4.66	8.137	10.748	1.4	< 0.50	30.0	1.2	0.388
	GW-03	43.0		4.56	0.357	1.185	3.1	< 0.50	15.0	4.3	1.255
	GW-04	56.0		2.85	0.348	2.031	2.9	< 0.50	7.3	1.4	0.790
	GW-05	23 (Offset = 16)		5.16	0.006	< 0.300	2.1	< 0.50	42.0	10.0	0.201
	GW-01B	0.0	Deep	4.92	N.D	< 0.300	1.2	< 0.50	9.3	17.0	< 0.100
	GW-02B	25.0		5.32	0.014	< 0.300	2.2	< 0.50	23.0	9.1	< 0.100
	GW-03B	43.0		5.90	0.353	1.604	2.7	< 0.50	26.0	< 0.5	0.404
	GW-04B	56.0		4.51	0.014	< 0.300	1.6	< 0.50	204.0	9.5	0.163
Transect 02	GW-10	0.0 (Offset = 17)	Shallow	4.97	0.033	< 0.300	1.8	< 0.50	22.0	6.6	< 0.100
	GW-11	13.0		4.83	0.039	0.511	1.8	< 0.50	6.2	4.8	0.219
	GW-12	33.0		4.62	0.284	1.157	1.9	< 0.50	20.0	3.3	0.593
	GW-13	48.0		4.31	15.577	29.375	2.5	< 0.50	15.0	4.6	0.199
	GW-14	41 (Offset = 14)		4.62	0.001	< 0.300	0.7	< 0.50	35.0	3.9	0.101
	GW-15	67 (Offset = 18)		4.68	0.009	< 0.300	3.9	< 0.50	28.0	31.0	< 0.100
	GW-11B	13.0	Deep	4.40	0.003	< 0.300	1.6	3.00	12.0	8.8	< 0.100
	GW-12B	33.0		5.28	0.002	< 0.300	1.9	< 0.50	43.0	12.0	< 0.100
	GW-13B	48.0		4.57	16.381	18.096	2.3	< 0.50	12.0	4.3	0.407
	GW-14B	41 (Offset = 14)		4.70	N.D	< 0.300	2.8	< 0.50	50.0	15.0	< 0.100
	GW-15B	67 (Offset = 18)		4.65	0.009	< 0.300	5.4	< 0.50	36.0	35.0	< 0.100

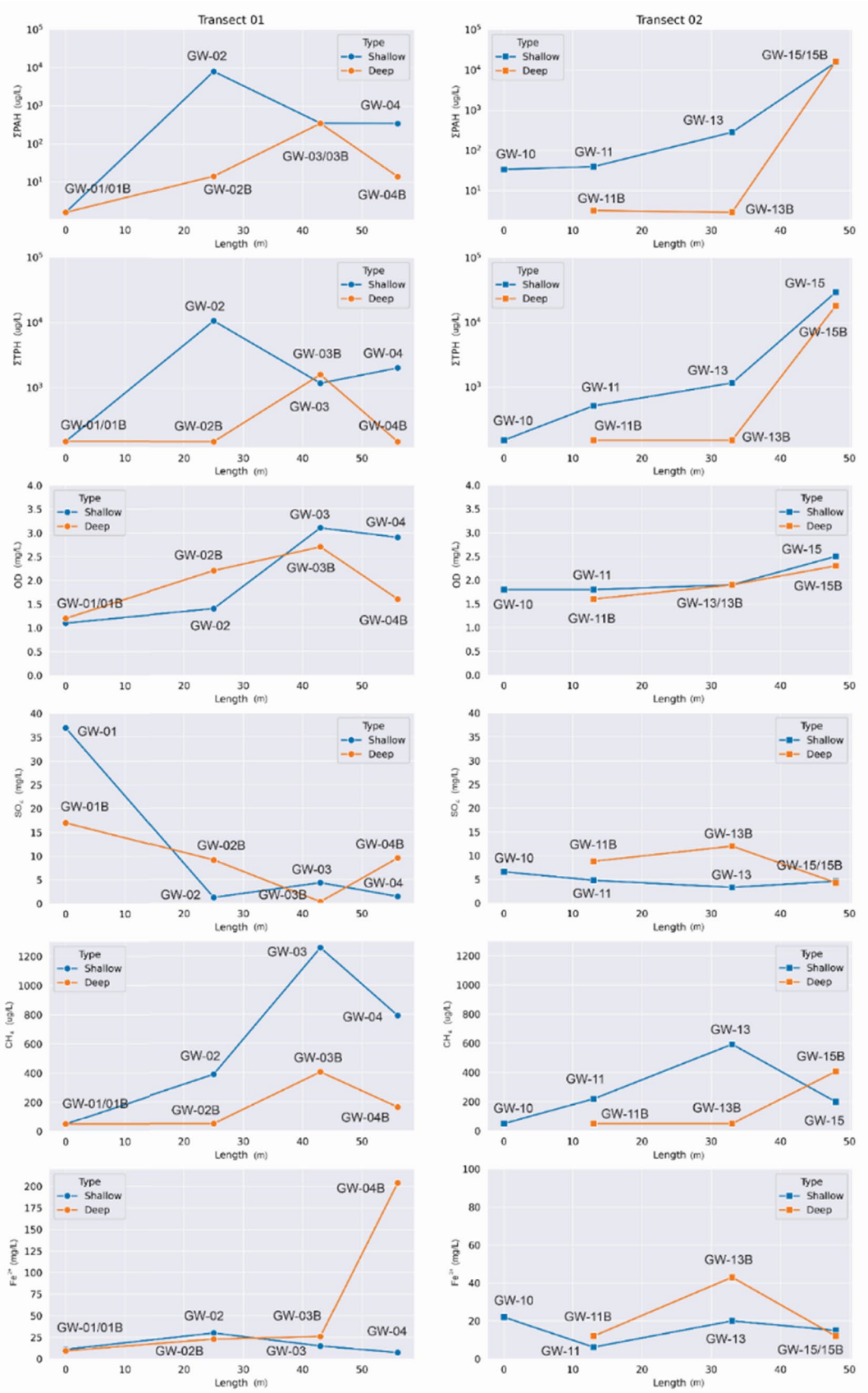

Fig. 9 Behavior of ΣPAH and ΣTPH concentrations in groundwater along transects 1 and 2, not considering the offset clusters

greater migration through the strata, resulting in a deeper distribution of the contaminants. In addition, the analysis of geochemical parameters and natural attenuation processes indicated that the Source 1 area, associated with wells GW-12 and GW-12B, is subject to active degradation processes, mainly due to the availability of electron acceptors and microbial competition, which contributes to the classification of this area as a significant source of contamination, even though the contaminant concentrations at depth are lower.

The dissolved oxygen (DO) concentrations observed along the transects were lower than expected for the groundwater in the perched aquifer, with an increase in its concentration as the distance from Source 1 increased. Low concentrations of DO are an indicator of consumption resulting from the decomposition of organic compounds originating from natural or anthropogenic sources. Due to the shallower position of the perched aquifer, it is more susceptible to physicochemical changes. On the other hand, with the increase in distance from the source zones, and reduction of hydrocarbon concentrations, an increase in the concentrations of dissolved oxygen in the offset monitoring wells was observed. Suggesting that the reduction in DO is caused by anthropogenic impact, also occurring in places upstream of the study area (Fig. 9).

The results of dissolved oxygen, nitrate (NO_3), iron (Fe^{2+}), sulfate (SO_4), and methane (CH_4) denote the presence of biochemical signatures of polycyclic aromatic hydrocarbons and total petroleum hydrocarbons degradation processes in groundwater, indicating that the area is under active natural attenuation processes occurring via several simultaneous routes, this zonation is likely the result of availability of electron acceptors and the competition of microorganisms of electron acceptors. The only sample that presented concentrations of NO_3 (3.0 mg/L) was the one collected in the GW-11B monitoring well. The absence of NO_3 in the solution suggests that the denitrification process is not occurring or has ended, with nitrate used as the initial priority electron acceptor. Sites with plumes of dissolved total petroleum hydrocarbons generally do not contain nitrate due to the rapid adaptation of the bacterial population and the preferred degradation routes are determined by the type of electron acceptor available, usually initiated by denitrification [26]. The evaluation of the routes presented in the conceptual model of geochemical evolution (Fig. 10), indicates the occurrence of iron (III) and sulfate reduction processes, as well as methanogenesis, evidenced by the presence of their electron acceptors and by-products.

While methane concentrations prevail in the zones that are closest to the sources, the decrease concentration of SO_4 (sulfate reduction) and the Fe^{2+} concentration increasing (Fe III reduction) are observed in the wells furthest from the sources and offset monitoring wells, as well as in the most peripheral areas of the plumes, which corroborates the typical distribution of anaerobic terminal electron-accepting processes of groundwater contamination by total

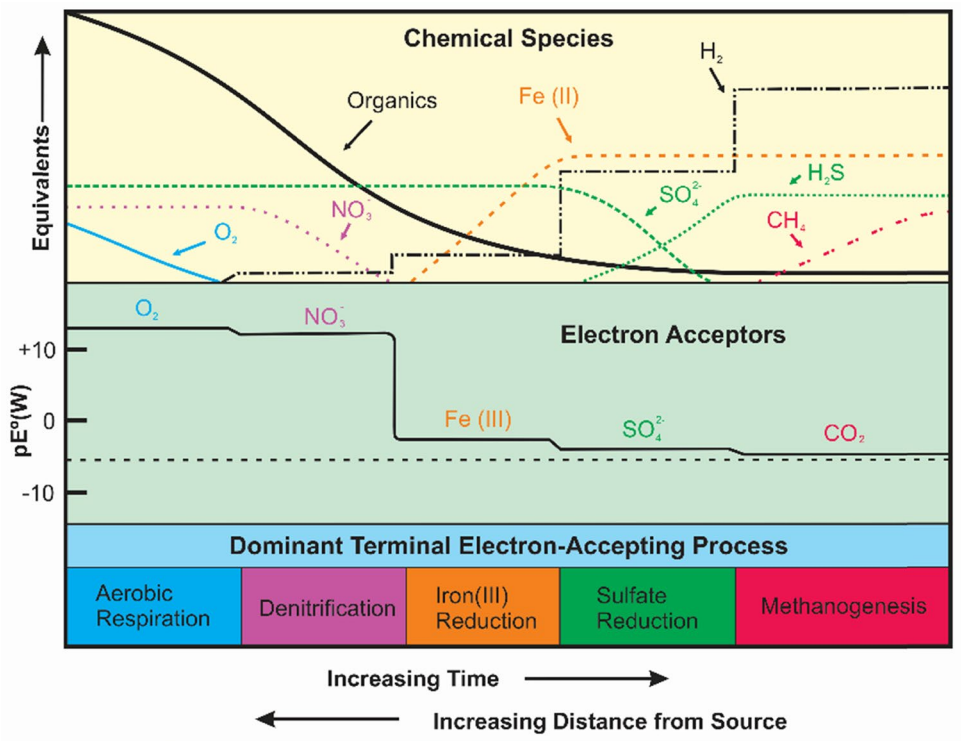

Fig. 10 Conceptual model of the geochemical evolution of groundwater contaminated by hydrocarbons (adapted from [70])

petroleum hydrocarbons and polycyclic aromatic hydrocarbons. If Fe (III) or sulfate are available, methanogenesis is generally excluded because Fe (III) reducers and sulfate reducers are able to outcompete the methanogenic community for electron donor [71]. Local environmental characteristics will determine the dominant process and the availability of hydrocarbons in solution. In this way, temporal and spatial variations of the dominant degradation process are expected. The methane concentrations in transects 1 and 2 increase after the area of Source 1, suggesting that, due to the proximity of the sampling points, the monitoring wells in transect 2 are under the influence of the contamination plume generated by Source 1. The behaviour of methane concentrations indicates the occurrence of methanogenesis, associated with the proximity of the source areas, which present lower dissolved oxygen, and favor the anaerobic hydrocarbon degradation.

The assessment of degrading biological activity of polycyclic aromatic hydrocarbons and metagenomic classification identified 50 genera divided into seven classes in the BIO01 sample: Actinobacteria, Alphaproteobacteria, Bacilli, Bacteroidia, Clostridia, Desulfovibrionia, Gammaproteobacteria, Halanaerobiia, Synergistia, and Thermotogae. The dominant presence was identified as Halanaerobium (Table 4), an obligate anaerobic halophile known for its complex fermentation of organic products and the production of intermediate metabolites for other trophic groups, such as sulfate-reducing bacteria and methanogenic bacteria [72]. Its prevalence in the sample is associated with the saturated, potassium-rich environment (arkosic sand), being a microorganism that thrives in high salt concentrations by accumulating cations like potassium and/or producing metabolites that aid in adapting to the environment. Another genus with significant occurrence was Pseudomonas. This facultative anaerobe is capable of degrading polycyclic aromatic hydrocarbons. In the absence of oxygen, it utilizes nitrate, sulfate, manganese (IV), iron (III), or carbon dioxide as alternative electron acceptors [73]. The degradation potential of polycyclic aromatic hydrocarbons and total petroleum hydrocarbons and BCP is also reported by [74–76].

The presence of all 16 priority PAHs was identified, with a concentration of ΣPAH16 = 379.88 mg/kg, suggesting that the diversity of identified microorganisms may be associated with the heterogeneity and diversity of polycyclic aromatic hydrocarbon compounds constituting the contamination. The results of metagenomic classification highlight the occurrence of polycyclic aromatic hydrocarbon-degrading genera and other hydrocarbon molecules, validating the observations made in groundwater samples. This corroborates [21], who identified variations in magnetic susceptibility in contaminated soil samples in the UTM Jaguaré area, indicating the presence of ultrafine magnetic particles related to extracellular biogenic processes containing iron. As pointed out by [77], there is no evidence that the natural attenuation process of polycyclic aromatic hydrocarbons occurs under specific geochemical conditions; it can occur simultaneously in microaerophilic regions interspersed with anaerobic regions or sulfidogenic regions interspersed with ferrogenic regions.

When assessing both the analytical results and the geochemical evolution in the study area's flowline, it is important to consider that there is a multi-component aged contamination, with the presence of total petroleum hydrocarbons and PAH (aliphatic and aromatic hydrocarbons). The substances with a lower molecular weight are partitioning and biodegraded more quickly, altering the dynamics of the known natural attenuation cycles, with overlapping phases due to the different stages of solubilization, as well as biochemical interactions to which organic molecules are subjected in the environment. Polycyclic aromatic hydrocarbons compounds can have a low molecular weight (two or three rings) or a high molecular weight (four rings or more). When introduced into the environment, these properties affect the degradation potential of polycyclic aromatic hydrocarbons by natural attenuation, as well as their sorption in mineral and organic fractions. The higher the molecular weight, the more recalcitrant the molecule becomes, a characteristic that has a slowing effect on the attenuation process due to the gradual release of compounds, producing long-lasting contamination that can remain in the environment for decades [26, 78].

Table 4 Metagenomic classification and counting of prioritized genera identified in the BIO01 sample

Genus	BIO01	
	Count	%
Halanaerobium	37,414	58.40
Pseudomonas	18,410	28.74
Pantoea	2612	4.08
Ralstonia	1135	1.77
Burkholderia-Caballeronia-Paraburkholderia	761	1.19

6 Discussions and interpretations

The results from the granulometric characterization and electrical logging were analyzed to assess how textural variation affects the acquisition of electrical conductivity logging data. This analysis verified the method's sensitivity to profiles with heterogeneous layers and its capability to differentiate small textural changes, which were noted during the visual tactile description. The correlation between clay content and the electrical conductivity recorded in the profile was good, as the behavior of the electrical conductivity log aligned well with the distribution and thickness of the described layers (Figs. 11 and 12). The dipole array utilized in the MH6534 probe successfully identified clay lenses along the driving Section (5.87 to 6.0 m; 7.00 to 7.05 m), with thicknesses ranging from 0.05 to 0.13 m. Consequently, this illustrates that the electrical conductivity profiling technique possesses sensitivity for acquiring and discretizing stratigraphic data, even in the presence of thin layers, supporting the findings reported by [44]. The variations in natural gamma ray counts with depth provided information consistent with the interpretations of the electrical logging results. Especially in GW-10, GW-12 and GW-15 loggings, the gamma ray count values increased at the contact of Unit 02 (clay) and Unit 03 (poorly sorted sand). The increase in gamma ray count is associated with the considerable presence of potassium feldspars in the typical sandy layer of this tropical soil, resulting in the observed decrease in electrical conductivity in the logging. Although the results of both methodologies were obtained in the saturated layer, below the water table, the water filling in the pores of the sandy soil was not sufficient to prevent contrast with Unit 02 of clayey composition and therefore with more conductive electrical properties.

Variations in natural gamma ray counts and electrical conductivity values were also important for the stratigraphic classification of the superficial layer of the contaminated area (Figs. 11 and 12). Although Unit 1 is not very thick, the layer exhibited material typical of a landfill, characterized by highly heterogeneous material. This included the presence of anthropogenic materials deposited in the area. The variations in the gamma signal in this unit were not as relevant when compared with the description of the geological borehole and the results of electrical profiling.

This made it difficult to determine the presence of important geological structures in a study of contaminant behavior in the physical environment, such as the presence of clay lenses. However, variations in electrical conductivity were observed in this unit. This possibly occurs because electrical logging is more sensitive to changes in the physical environment. It is therefore interesting to use the two methodologies together, so that one investigation technique complements

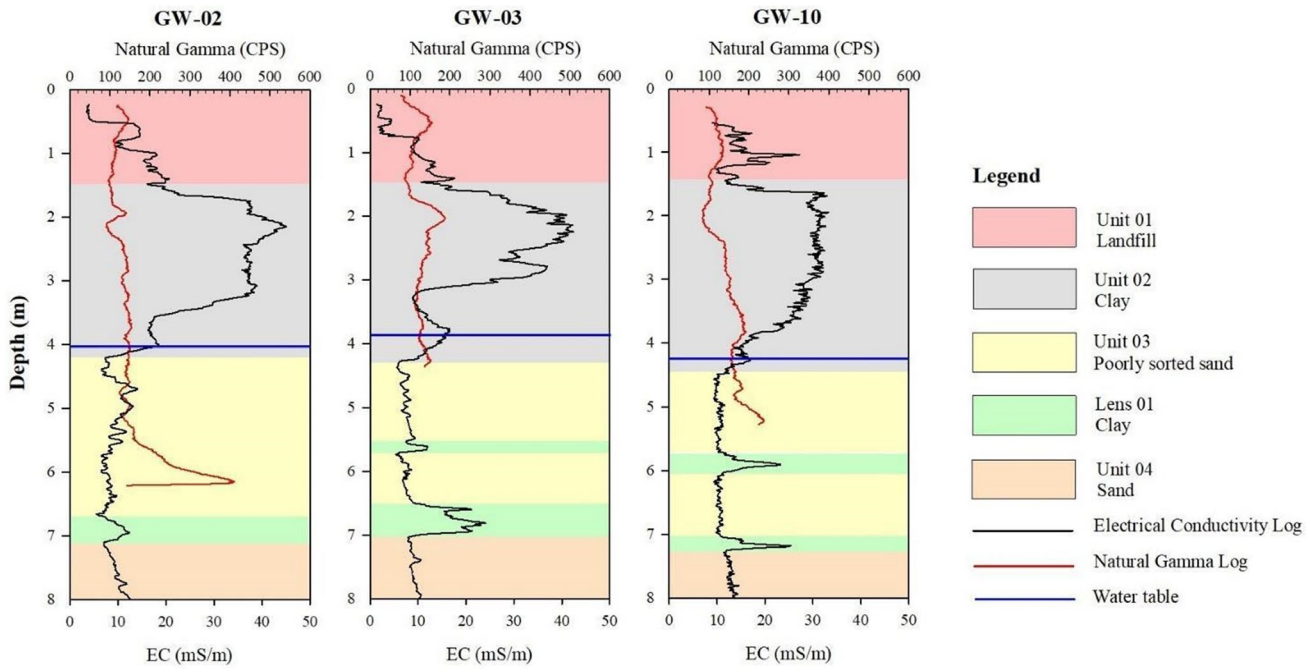

Fig. 11 Integrated analysis of the tests carried out at the sampling points in transect 1, including stratigraphic, electrical conductivity, gamma-ray logging, and water level data. It is possible to observe variations in physical parameters at the contact between units of distinct granulometric compositions

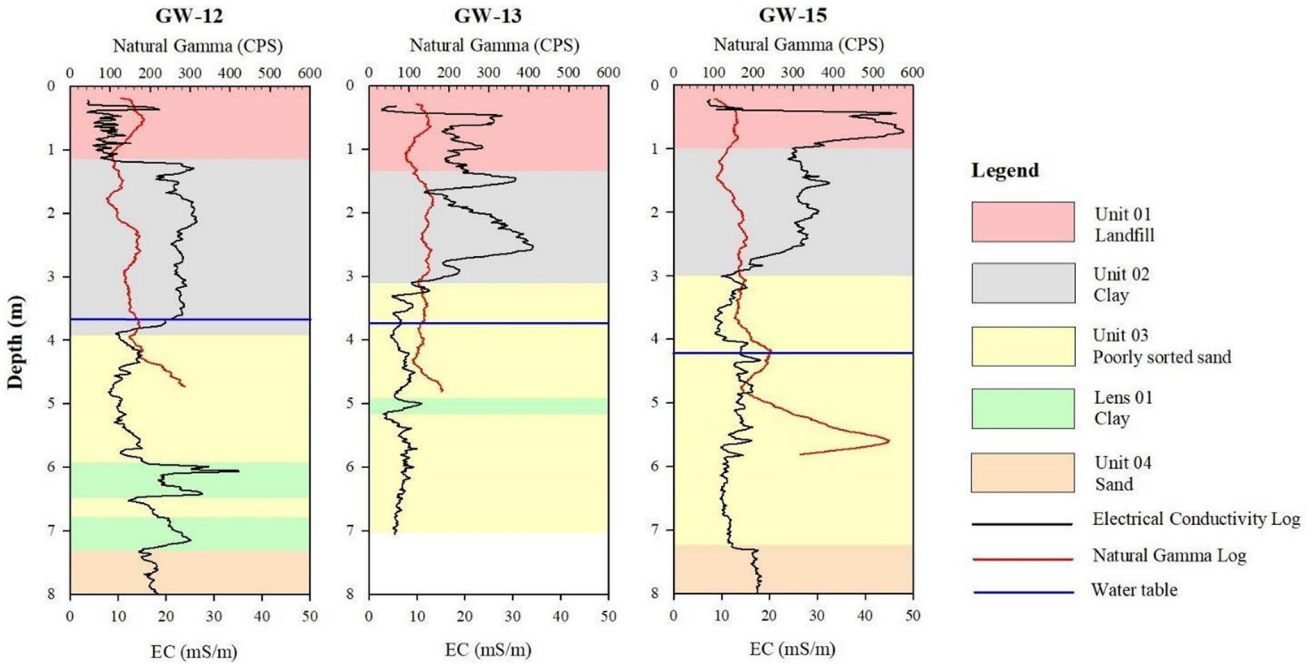

Fig. 12 Integrated analysis of the tests carried out at the sampling points in transect 2, including stratigraphic, electrical conductivity, gamma-ray logging, and water level data. It is possible to observe variations in physical parameters at the contact between units of distinct granulometric compositions

the limitations of the other and results in a good stratigraphic characterization of the contaminated area. However, when analyzing the indirect characterization data at different sampling points (bottom, contaminated area and offset) (Fig. 13), it can be seen that the variation in the gamma signal in Unit 3 is more evident at the edges of the plumes and in nearby regions (offset monitoring well), where lower concentrations of contaminants are identified, creating a favorable environment for the stabilization and development of the microbial community. The dispersion analysis of the natural gamma ray counts and electrical conductivity values for Units 1, 2 and 3 were compared at different depths. The variations in gamma ray emissions per second may be associated with the presence of contaminants at depth. These variations suggest that the natural attenuation of hydrocarbon contamination is triggering biogeochemical changes, causing the dissolution of potassium in feldspar minerals present in local arcosian sands. In this way, potassium in solution is being

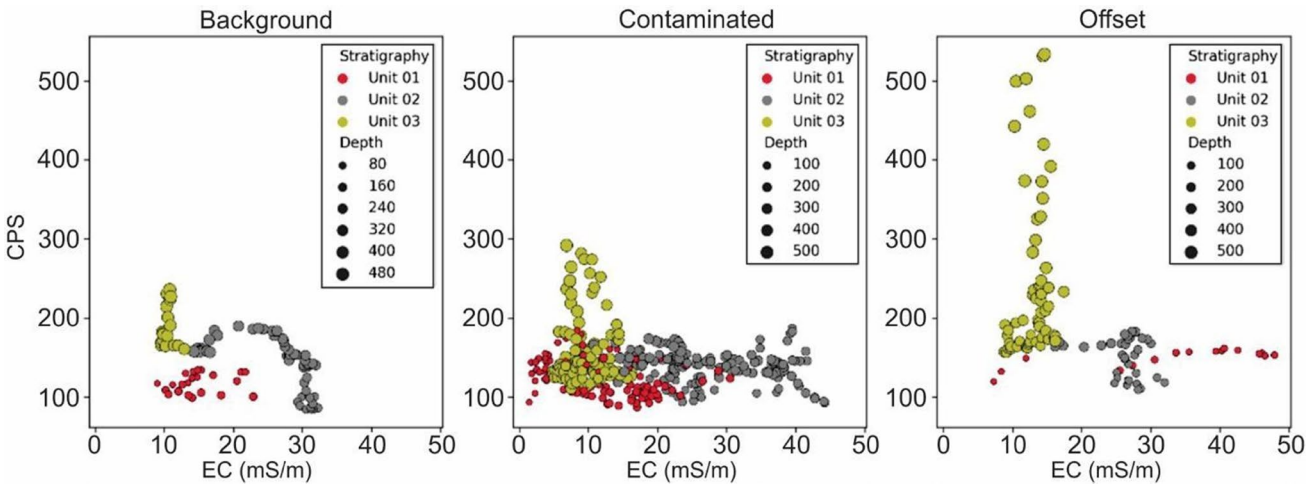

Fig. 13 Dispersion analysis of natural gamma ray counts (CPS) and electrical conductivity (EC) variables in Units 1, 2 and 3 at depth

remobilized to greater depths in the unsaturated zone. The geochemical changes were supported by chemical analyses of the groundwater in the study area.

This suggests that the natural attenuation of hydrocarbon contamination, as evidenced by the chemical analysis and metagenomic classification, is triggering biogeochemical changes that are causing potassium to dissolve in the feldspar minerals present in the arcosian sands that make up the local mineralogy. The high mobility of potassium in solution leads to its remobilization at greater depths, which was evidenced by the gamma signal values recorded. Redox reactions mediated by microorganisms can alter the stability of minerals, promoting their dissolution and mobilization [79, 80]. The same results were observed by [20], when they showed the chemical weathering generated by biological activity in the solid fraction of a soil contaminated with hydrocarbons, resulting from natural attenuation processes. As the gamma profiles are associated with pre-existing monitoring wells, in order to obtain more comprehensive data, it is necessary to carry out larger studies, covering greater distances from the source of contamination, with analyses inside and outside the area of the contamination plume, making it possible to assess the extent of the effects of the presence of total petroleum hydrocarbons and total polycyclic aromatic hydrocarbons on the geochemical alterations of the environment.

7 Conclusions

The presence of hydrocarbon contaminants in soil and groundwater directly affects biogeochemical processes, which are dependent on exposure time, stratigraphic architecture, and local, climatic, and geological dynamics, increasing the complexity of the analysis of natural attenuation processes. In this study, we found that:

1. Indirect and non-invasive methods proved to be a good alternative for obtaining data and understanding mineralogical and stratigraphic variations in detail in the area contaminated by hydrocarbons, in a complex hydrogeological context. Although natural gamma ray logging is not a geophysical method widely used in environmental contamination studies, the results obtained by the method revealed variations in the counts of gamma ray emissions per second, which helped to identify a typical floodplain stratigraphy, made up of layers of clay and sand, resulting from the frequent flooding of the river.
2. Granulometric variations and the results of the electrical conductivity profiles showed a good correlation. Values above 20 mS/m were observed for the clay layers and values below 15 mS/m for the sandy layers. Two peaks were observed in the electrical conductivity values, which may be associated with the presence of clay lenses in the subsurface. The identification of clay lenses in environmental remediation studies of contaminated areas is very important, as the geological material directly interferes with the direction and velocity of contaminant percolation in the physical environment. The results showed that the sensor-probe array was sensitive and capable of identifying small variations in a complex environment, such as the study area, characterized by changes in flood conditions, currents and sediment transport over time.

Author contributions AMB: Writing—original draft, Visualization, Validation, Supervision, Methodology, Investigation, Formal analysis, Data curation, Conceptualization. LGN: Writing—review & editing, Writing—original draft, Visualization, Validation, Supervision, Software, Formal analysis. CCG: Writing—review & editing, Writing—original draft, Visualization, Validation, Supervision, Software, Resources, Methodology, Investigation, Formal analysis, Data curation, Conceptualization. JPSP: Formal analysis, Data curation, Conceptualization. OCBG: Methodology, Investigation, Formal analysis, Data curation. LCRS: Methodology, Investigation. CAON: Validation, Supervision, Conceptualization.

Funding No funding was received.

Data availability The datasets generated during and/or analysed during the current study are available from the corresponding author on reasonable request.

Declarations

Competing interests The authors declare no competing interests.

References

1. Brazilian Institute of Geography and Statistics – IBGE. 2011. CENSO DEMOGRÁFICO - 2010. Características da população e dos domicílios: resultados do universo. Rio de Janeiro: IBGE, 2011. Acompanha 1 CD-ROM. https://www.ibge.gov.br/estatisticas/sociais/populacao/9662-censo-demografico-010.html?=&t=destaques. Acess in: set.2021.
2. Kemper RV. Rural-urban migration in Latin America: a framework for the comparative analysis of geographical and temporal patterns. Int Migr Ver. 1971;5(1):36–47. https://doi.org/10.2307/3002045.
3. Environmental Sanitation Technology Company—CETESB. Relatório de Áreas Contaminadas e Reabilitadas no Estado de São Paulo (2018). São Paulo, 2018.
4. Mondelli G, Giacheti HL, Boscov MEG, Elis VR, Hamada J. Geoenvironmental site investigation using different techniques in a municipal solid waste disposal site in Brazil. Environ Geol. 2007. https://doi.org/10.1007/s00254-006-0529-1.
5. Andersen TR, Poulsen SE, Alberdi-Pagola M, Medhus A. Geophysical mapping and 3D geological modeling to support urban planning: a case study from Vejle, Denmark. J Appl Geophys. 2020. https://doi.org/10.1016/j.jappgeo.2020.104130.
6. Guireli Netto L, Barbosa AM, Galli VL, Silva Pereira JP, Gandolfo OCB, Birelli CA. Application of invasive and non-invasive methods of geo-environmental investigation for determination of the contamination behavior by organic compounds. J Appl Geophys. 2020. https://doi.org/10.1016/j.jappgeo.2020.104049.
7. Netto LG, Guimarães CC, Barbosa AM, Gandolfo OCB. Investigation of the contamination behavior in water and soil of an inactive dump from chemical analysis and geophysical method. Discov Geosci. 2024. https://doi.org/10.1007/s44288-024-00010-8.
8. Moreira CA, Helene LPI, Nogara P, Ilha L. Analysis of leaks from geomembrane in a sanitary landfill through models of electrical resistivity tomography in South Brazil. Environ Earth Sci. 2017. https://doi.org/10.1007/s12665-017-7180-x.
9. Guireli Netto L, Guimarães CC, Barbosa AM, Gandolfo OCB. Characterization of an inactive dumpsite using electrical resistivity tomography and hydrochemical data: a case study in Brazil. Environ Earth Sci. 2023;82:529. https://doi.org/10.1007/s12665-023-11233-2.
10. Sauck WA. A model for the resistivity structure of LNAPL plumes and their environs in sandy sediments. J Appl Geophys. 2000. https://doi.org/10.1016/S0926-9851(99)00021-X.
11. Ustra AT, Elis VR, Mondelli G, Zuquette L, Giacheti HL. Case study: a 3D resistivity and induced polarization imaging from downstream a waste disposal site in Brazil. Earth Sci Res J. 2011. https://doi.org/10.1007/s12665-011-1284-5.
12. Flores Orozco A, Kemna A, Oberdörster C, Zschornack L, Leven C, Dietrich P, Weiss H. Delineation of subsurface hydrocarbon contamination at a former hydrogenation plant using spectral induced polarization imaging. J Contam Hydrol. 2012. https://doi.org/10.1016/j.jconhyd.2012.06.001.
13. Elis VR, Ustra A, Hidalgo-Gato MC, Pejon OJ, Hiodo FY. Application of induced polarization and resistivity to the environmental investigation of an old waste disposal area. Environ Earth Sci. 2016. https://doi.org/10.1007/s12665-016-6157-5.
14. Helene LPI, Moreira CA, Bovi RC. Identification of leachate infiltration and its flow pathway in landfill by means of electrical resistivity tomography (ERT). Environ Monit Assess. 2020. https://doi.org/10.1007/s10661-020-8206-5.
15. Guireli Netto L, Malagutti Filho W, Moreira CA, di Donato FT, Helene LPI. Delineation of necroleachate pathways using electrical resistivity tomography (ERT): Case study on a cemetery in Brazil. Environ Chall. 2021;5: 100344. https://doi.org/10.1016/j.envc.2021.100344.
16. Kress W, Teeple A. Two-dimensional resistivity investigation of the North Cavalcade Street Site, Houston, Texas, August 2003. Scientific Investigations Reports 2005; U.S. Geological Survey.
17. Cardarelli E, Di Filippo G. Electrical resistivity and induced polarization tomography in identifying the plume of chlorinated hydrocarbons in sedimentary formation: a case study in Rho (Milan - Italy). Waste Manag Res. 2009;27(6):595–602. https://doi.org/10.1177/0734242X09102524.
18. Koroma S, Arato A, Godio A. Analyzing geophysical signature of a hydrocarbon-contaminated soil using geoelectrical surveys. Environ Earth Sci. 2015;74:2937–48. https://doi.org/10.1007/s12665-015-4326-6.
19. Atekwana EA, Sauck WA, Werkema DD. Investigations of geoelectrical signatures at a hydrocarbon contaminated site. J Appl Geophys. 2000. https://doi.org/10.1016/S0926-9851(98)00033-0.
20. Abdel AGZ, Slater LD, Atekwana EA. Induced-polarization measurements on unconsolidated sediments from a site of active hydrocarbon biodegradation. Geophys. 2006;71:H13–24. https://doi.org/10.1190/1.2187760.
21. Moraes CS, Ustra AT, Barbosa AM, Aparecida RLI, Uehara CMT. Magnetic signatures of a creosote oil contaminated site: case study in São Paulo, Brazil. Sci Rep. 2022;12:21853. https://doi.org/10.1038/s41598-022-23493-2.
22. Godsy EM, Goerlitz DF, Grbic-Galic D. Methanogenic biodégradation of creosote contaminants in natural and simulated ground-water ecosystems. Groundwater. 1992;30:232–42. https://doi.org/10.1111/j.1745-6584.1992.tb01795.x.
23. Sharak Genthner BR, Townsend GT, Lantz SE, Mueller JG. Persistence of polycyclic aromatic hydrocarbon components of creosote under anaerobic enrichment conditions. Arch Environ Contam Toxicol. 1997;32:99–105. https://doi.org/10.1007/s002449900160.
24. Júlio ADL, Silva UCM, Medeiros JD, Morais DK, Santos VL. Metataxonomic analyses reveal differences in aquifer bacterial community as a function of creosote contamination and its potential for contaminant remediation. Sci Rep. 2019;9:1–14. https://doi.org/10.1038/s41598-019-47921-y.
25. Smułek W, Sydow M, Zabielska-Matejuk J, Kaczorek E. Bacteria involved in biodegradation of creosote PAH—a case study of long-term contaminated industrial area. Ecotoxicol Environ Saf. 2020;15(187): 109843. https://doi.org/10.1016/j.ecoenv.2019.109843.

26. Wiedemeier TH, Swanson MA, Moutoux DE, Wilson JT, Kampbell DH, Hansen JE, Haas P. Overview of the technical protocol for natural attenuation of chlorinated aliphatic hydrocarbons in ground water under development for U.S. Air Force Center for environmental excellence. 37–61. U.S. EPA. Proceedings of Symposium on natural attenuation of chlorinated organics in ground water. Washington DC, USA, 1997. Accessed 12 Jan 2024.
27. Schmutz M, Blondel A, Revil A. Saturation dependence of the quadrature conductivity of oil-bearing sands. Geophys Res Lett. 2012;39:L03402. https://doi.org/10.1029/2011GL050474.
28. Mewafy F, Werkema D, Atekwana EA, Slater L, Abdel AG, Ntarlagiannis D. Evidence that bio-metallic mineral precipitation enhances the complex conductivity response at a hydrocarbon contaminated site. J Appl Geophys. 2013;98:113–23. https://doi.org/10.1016/j.jappgeo.2013.08.011.
29. Kimak C, Ntarlagiannis D, Slater LD, Atekwana EA, Beaver CL, Rossbach S, Porter A, Ustra A. Geophysical monitoring of hydrocarbon biodegradation in highly conductive environments. J Geophys Res-Biogeo. 2019. https://doi.org/10.1029/2018JG004561.
30. Goldenstein L, Rossini RE. O bairro industrial do Jaguaré, SP. São Paulo: Boletim Paulista de Geografia, n. 47, 30–72 p, 1972.
31. Mueller JG, Chapman PJ, Prichard PH. Creosote-contaminated sites: their potential for bioremediation. Environ Sci Technol, 1989; 1197–1201 p.
32. IPT, Instituto de Pesquisas Tecnológicas. Investigação detalhada—Área da Antiga Unidade de Tratamento de Madeiras Jaguaré, bairro Jaguaré. São Paulo—SP. São Paulo: IPT, 2019.
33. Brasil. Ministério do Meio Ambiente (MMA). Conselho Nacional do Meio Ambiente (CONAMA). Resolução CONAMA Nº 420, de 08/12/2009. Dispõe sobre critérios e valores orientadores de qualidade do solo quanto à presença de substâncias químicas e estabelece diretrizes para o gerenciamento ambiental de áreas contaminadas por essas substâncias em decorrência de atividades antrópicas.
34. Aranha RM, Magalhães VMA, Paupitz GM, Soares LCR, Barbosa AM, Nascimento CAO, Vianna MGR, Chiavone-Filho O. Characterization and partitioning behavior of creosote in different matrices: soil, water, and air. Water Air Soil Pollut. 2020. https://doi.org/10.1007/s11270-020-04772-y.
35. PMSP. Estudo mapeamento digital da cidade de São Paulo do ano de 2004. Disponível em http://geosampa.prefeitura.sp.gov.br/), 2004; Accessed 05 Nov 2023.
36. Monteiro MD, Gurgueira MD, Rocha HC. Geologia da Região Metropolitana de São Paulo. In: Twin cities: solos das regiões metropolitanas de São Paulo e Curitiba. NEGRO, Ars ed. São Paulo. p. 512, 2012.
37. Perrotta MM, Salvador ED, Lopes RC, D'agostino LZ, Chieregati LA, Peruffo N, Gomes SD, Sachs LLB, Meira VT, Garcia MGM, Lacerda Filho JV. Geologia e recursos minerais do estado de São Paulo: Sistema de Informações Geográficas - SIG. Rio de janeiro: CPRM, 2006.
38. Riccomini C, Coimbra AM. Geologia da bacia sedimentar. In Solos da cidade de São Paulo. Ferreira AA, Alonso UR, Luz PL, editors. São Paulo, ABMS/ABEF, 1992, p 37–94. Accessed 14 Nov 2023.
39. Iritani MA. Potencial hidrogeológico da Cidade Universitária de São Paulo. (Dissertação de Mestrado), Departamento de Geologia Econômica, Instituto de Geociências, Universidade de São Paulo, 1993, 97p. Accessed 20 Jan 2024.
40. Rodriguez SK. Geologia urbana da região metropolitana de São Paulo. Tese de Doutorado, Instituto de Geociências, Universidade de São Paulo, 1998, São Paulo. https://doi.org/10.11606/T.44.1998.tde-19112015-093141.
41. ASTM International. D6282/D6282M-14 Standard guide for direct push soil sampling for environmental site characterizations. West Conshohocken, PA; ASTM International, 2014. https://doi.org/10.1520/D6282_D6282M-14.
42. De Lemos RC, dos Santos RD. Manual de descrição e coleta de solo no campo 2 ed. Campinas: Sociedade Brasileira de Ciência do Solo; Rio de Janeiro. EMBRAPA-SNLCS, 46 p, 2013.
43. ABNT NBR 7181:2018. Solo—Análise granulométrica. ABNT—Associação Brasileira de Normas Técnicas. Rio de Janeiro, 2018. 12 p.
44. Christy CD, Christy TM, Wittig V. A percussion probing tool for the direct sensing of soil conductivity. Technical Paper Nº 94–10, Geoprobe System. 1994.
45. Geoprobe. Geoprobe Membrane Interface Probe (MIP) Standard Operating Procedure. Technical Bulletin no MK3010. Revised January, 2015. Accessed 12 Jan 2024.
46. Schulmeister MK, Butler JJ Jr, Healey JM, Zheng L, Wysocki DA, Mccall GW. Direct-push electrical conductivity logging for high-resolution hydrostratigraphic characterization. Ground Water Monit Remediat. 2003;23:52–62. https://doi.org/10.1111/j.1745-6592.2003.tb00683.x.
47. Parasnis DS. Principles of applied geophysics, 5th edn. Chapman & Hall, New York, 429p, 1997.
48. Telford WM, Geldart LP, Sheriff, RE. Applied Geophysics. Cambridge Univ. Press., 2nd edn, 770 p, 1990. Accessed 10 Jan 2024.
49. ASTM D7352-07, Standard practice for direct push technology for volatile contaminant logging with the Membrane Interface Probe (MIP), ASTM International, West Conshohocken, PA, 2007, https://doi.org/10.1520/D7352-07.
50. Asquith G, Krygowski D, Henderson S, Hurley N. "Gamma Ray Log", Basic well log analysis, George Asquith, Daniel Krygowski, Steven Henderson, American Association of Petroleum Geologists, Neil Hurley. 2004; https://doi.org/10.1306/Mth16823.
51. Diaz-Curiel J, Miguel MJ, Biosca B, Arevalo-Lomas L. Gamma ray log to estimate clay content in the layers of water boreholes. J Appl Geophys. 2021. https://doi.org/10.1016/j.jappgeo.2021.104481.
52. Rider M. The geological interpretation of wireline logs. Whittles, Caithness, 1996. Accessed 12 Dec 2023.
53. Hampson GJ, Davies W, Davies SJ, Howell JA, Adamson KR. Use of spectral gamma-ray data to refine subsurface fluvial stratigraphy: late Cretaceous strata in the Book Cliffs, Utah, USA. J Geol Soc London. 2005;162:603–21.
54. Tzortzis M & Tsertos H. Gamma-ray measurements of naturally occurring radioactive samples from Cyprus characteristic geological rocks, UCYPHY 02/02. Cyprus: Department of Physics, University of Cyprus, 2002. Accessed 21 Nov 2023.
55. Franchini S, De Filippi FM, Barbieri M, Sappa G. γ-Ray log tool for detecting the presence of low-permeability lenses in high-resolution modelling of contaminated sites. Water. 2023. https://doi.org/10.3390/w15203590.
56. U.S. EPA. Method 300.1: Determination of inorganic anions in drinking water by ion chromatography. Revision 1.0. Cincinnati, OH, 1997. Accessed 08 Jan 2024.
57. Standard Methods For the Examination of Water and Wastewater—SMWW (2017). 4500-O OXYGEN (DISSOLVED). American Public Health Association. https://doi.org/10.2105/SMWW.2882.091.
58. Standard Methods For the Examination of Water and Wastewater—SMWW (2017). 3500-Fe IRON. American Public Health Association. https://doi.org/10.2105/SMWW.2882.055.

59. U.S. EPA. Method 8015C (SW-846): Nonhalogenated Organics Using GC/FID. Revision 4. Washington, DC, 2003. Accessed 08 Jan 2024.
60. EPA. Method 8260C (SW-846): Volatile Organic Compounds by Gas Chromatography/Mass Spectrometry (GC/MS). Revision 3, 2006. Accessed 05 Dec 2023.
61. U.S. EPA. Method 8015C (SW-846): Nonhalogenated Organics Using GC/FID. Revision 4. Washington, DC. 2003.
62. U.S. EPA. Method 8260D (SW-846): volatile organic compounds by gas chromatography/mass spectrometry (GC/MS). Revision 3. Washington, DC. 2006.
63. Callahan BJ, et al. DADA2: high resolution sample inference from Illumina amplicon data. Nat Methods. 2016;13(7):581–3.
64. Klindworth A, Pruesse E, Schweer T, Peplies J, Quast C, Horn M, Glöckner FO. Evaluation of general 16S ribosomal RNA gene PCR primers for classical and next-generation sequencing-based diversity studies. Nucleic Acids Res. 2013;41(1):1.
65. Carvalho DLR. Indicadores geomorfológicos de mudanças ambientais no sistema fluvial do Alto Tietê (município de São Paulo): pesquisa documental. 2006. 2v. + anexos. Dissertação (Mestrado em Geografia Física) - Departamento de Geografia, FFLCH, USP, São Paulo. Accessed 10 Jan 2024.
66. IUSS Working Group WRB, 2015. Base referencial mundial del recurso suelo 2014, Actualización 2015. Sistema internacional de clasificación de suelos para la nomenclatura de suelos y la creación de leyendas de mapas de suelos. Informes sobre recursos mundiales de suelos 106. FAO, Roma.
67. Corwin DL, Lesch SM. Characterizing soil spatial variability with apparent soil electrical conductivity. Comput Electron Agric. 2005;46:103–33. https://doi.org/10.1016/j.compag.2004.11.002.
68. Serra O, Baldwin J, Quirein J. Theory, interpretation, and practical applications of natural gamma ray spectroscopy. Paper presented at the SPWLA 21st Annual Logging Symposium, Lafayette, Louisiana, 1980.
69. Fertl WH, Chilingarian GV, Yen TF. Use of natural gamma ray spectral logging in evaluation of clay minerals. Energy Sources. 1982;6(4):335–60. https://doi.org/10.1080/00908318208946036.
70. Bouwer EJ, McCarty PL. Modeling of trace organics biotransformation in the subsurface. Ground Water. 1984;22(4):433–40. https://doi.org/10.1111/j.1745-6584.1984.tb01414.x.
71. Lovley DR, Chapelle FH. Deep subsurface microbial processes. Rev Geophys. 1995;33:365–81.
72. Motlagh AM, Bhattacharjee AS, Coutinho FH, Dutilh BE, Casjens SR, Goel RK. Insights of phage-host interaction in hypersaline ecosystem through metagenomics analyses. Front Microbiol. 2017;8:352.
73. Liu Y, Hu H, Zanaroli G, Xu P, Tang H. A Pseudomonas sp. strain uniquely degrades PAHs and heterocyclic derivatives via lateral dioxygenation pathways. J Hazard Mater. 2021. https://doi.org/10.1016/j.jhazmat.2020.123956.
74. Goveas LC, Menezes J, Salian A, Krishnam A, Alva M, Basavapattan B, Sajankila SP. Petroleum hydrocarbon degradation in soil augmented with used engine oil by novel Pantoea wallisii SS2: optimisation by response surface methodology Louella. Biocatal Agric Biotechnol. 2020;25: 101614.
75. Purnomo AS, Rizqi HD, Harmelia L, Anggraeni SD, Melati RE, Damayanti ZH, Shafwah OM, Kusema FC. Biodegradation of crude oil by Ralstonia pickettii under high salinity medium. Mal J Fund Appl Sci. 2019;15(3):377–80.
76. Morya R, Salvachúa D, Thakur IS. Burkholderia: an untapped but promising bacterial genus for the conversion of aromatic compounds. Trends Biotechnol. 2020. https://doi.org/10.1016/j.tibtech.2020.02.008.
77. Rogers SW, Ong SK, Kjartanson BH, Golchin J, Stenback GA. Natural attenuation of polycyclic aromatic hydrocarbon-contaminated sites: review, practice periodical of hazardous. Toxic Radioact Waste Manag. 2002;6(3):141–55. https://doi.org/10.1061/(ASCE)1090-025X(2002)6:3(141).
78. Jacques RJS, Okeke BC, Bento FM, Peralba MCR, Camargo FAO. Improved enrichment and isolation of polycyclic aromatic hydrocarbons (PAH)-degrading microorganisms in soil using anthracene as a model PAH. Curr Microbiol. 2009;58(6):628–34.
79. Bennett PC, Hiebert FK, Choi WJ. Microbial colonization and weathering of silicates in petroleum-contaminated groundwater. Chem Geol. 1996;132:45–53. https://doi.org/10.1016/S0009-2541(96)00040-X.
80. Atekwana EA, Slater LD. Biogeophysics: a new frontier in earth science research. Rev Geophys. 2009;47:4004. https://doi.org/10.1029/2009RG000285.